Available online at www.sciencedirect.com
SCIENCE DIRECT®
Journal of Hydrology 309 (2005) 277–300
Journal of Hydrology
www.elsevier.com/locate/jhydrol

SiSPAT-Isotope, a coupled heat, water and stable isotope (HDO and $H_2^{18}O$) transport model for bare soil. Part I. Model description and first verifications

I. Braud[a,c,*], T. Bariac[b], J.P. Gaudet[a], M. Vauclin[a]

[a]LTHE (UMR 5564 CNRS, INPG, IRD, UJF), BP 53, 38041 Grenoble Cédex 9, France
[b]BIOMCO, UMR 7618 CNRS-UPMC-INRA, INRA-INAPG, Bâtiment EGER, 78850 Thieverval-Grignon, France
[c]Cemagref Unite de Recherche en Hydrologie-Hydraulique, 3 bis Quai Chauveau, CP 220, 69336 Lyon Cédex 9, France

Received 4 August 2003; revised 6 December 2004; accepted 21 December 2004

Abstract

Stable water isotopes, namely deuterium and oxygen 18, are tracers of water movement within the soil–vegetation–atmosphere system. They provide useful information for a better understanding of evaporation and transpiration processes as well as water vapour transport within soils. To better evaluate those potentialities and to identify possible lack of knowledge, a coupled heat, water and stable isotope transport model, called SiSPAT-Isotope was developed for bare soil. This paper presents the theoretical basis of the model, revisiting existing formulations encountered in the literature. An emphasis was put on the formulation of the kinetic fractionation factor, conditioning the resistance to isotope transport between the soil surface and the atmosphere, for which no agreement exists in the literature. The paper also presents first validation tests, showing the consistency of the model by comparison with existing analytical solutions. Sensitivity tests showed that the isotope concentration was very sensitive to the formulation of the resistance to isotope transport between the soil surface and the atmosphere, especially under saturated soil conditions. Only a comparison with existing data sets and further laboratory and field experiments, can help decide which formulation has to be used and in which conditions. Finally, an example of simulation under non-steady state conditions is also presented and discussed.
© 2005 Elsevier B.V. All rights reserved.

Keywords: Coupled heat; Water and stable isotope transport model; Resistance to isotope transfer; Kinetic fractionation factor

1. Introduction

Evaporation from soils and transpiration by vegetation represent the major rainfall-recycling source over continents. Consequently, a correct assessment of potential impacts of water management practices, land use and/or climate change on water resources relies on an accurate representation of

* Corresponding author. Address: Cemagref Unite de Recherche en Hydrologie-Hydraulique, 3 bis Quai Chauveau, CP 220, 69336 Lyon Cédex 9, France. Tel.: +33 4 72 20 87 78; fax: +33 4 78 47 78 75.
E-mail address: braud@lyon.cemagref.fr (I. Braud).

0022-1694/$ - see front matter © 2005 Elsevier B.V. All rights reserved.
doi:10.1016/j.jhydrol.2004.12.013

evapotranspiration within atmosphere, hydrological or vegetation growth models. The purpose of Soil Vegetation Atmosphere Transfer (SVAT) models is to represent complex interactions between the atmosphere, the soil and the biosphere. Most of them provide separate estimates of soil evaporation, interception by the canopy and transpiration by plants. However, few data (relying mainly on sap flow and micro-lysimeters measurements) are currently available to validate that partition. Concentration measurements of stable water isotopes in soils, in leaves and in the transpired and evaporated vapours provide an alternative way to quantify it (e.g. Yepez et al., 2003; Williams et al., 2004 for recent publications). Indeed, the liquid concentration is known to rise under soil evaporation, whereas no fractionation of isotopic forms of either oxygen or hydrogen occurs during root extraction (Zimmermann et al., 1967; Walker and Richardson, 1991; Bariac et al., 1994, 1995). Therefore, measurements of stable water isotopes concentration within the soil can provide useful information for (i) determining the depth at which plants are extracting water at a given time and therefore validate root extractions sub-models in SVATs and (ii) better quantifying water transfer within soils (mainly vapour diffusion coefficients and hydraulic properties).

A physically based model, representing the full interactions between the atmosphere, the soil, the vegetation and stable isotope species can provide a powerful tool for testing various hypotheses about active processes. As it also provides a synthesis of our current knowledge of these processes, it can help, when compared with observed data, to identify the gaps in knowledge and the points requiring further investigations. Those arguments motivated a modelling effort aimed at representing the coupled heat, water and stable isotope transport within the soil–vegetation–atmosphere continuum. The Simple Soil Plant Atmosphere Transfer (SiSPAT) model (Braud et al., 1995; Braud, 2000) was already simulating in details the soil–plant–atmosphere continuum interactions. It was therefore necessary to add a stable isotope transport module to the existing model in order to reach our goal. The work was, however, performed in two steps. The first one deals with bare soil and the second step will consider the vegetation. In this paper we focus on the bare soil isotope transfer module and describe the corresponding model formulation. A first evaluation of model calculations is performed using analytical solutions available from the literature under steady state conditions. Likelihood tests showing the qualitative agreement of the numerical simulations with the behaviour evidenced by data are also described. The comparison of model simulations with two experimental laboratory data sets is presented in Part II of this paper (Braud et al., 2004).

Section 2 presents a brief review of existing stable isotope transport modelling efforts. Section 3 shortly describes the existing SiSPAT SVAT model. Sections 4 and 5 present the stable isotope transport equation and upper boundary condition specification, respectively. An assessment of the accuracy of the numerical model is given in Section 6 using a comparison with analytical solutions. We also present sensitivity tests to the formulation of the surface isotope flux. Finally, Section 7 provides an example of a non-steady state simulation, before drawing some conclusions.

2. Modelling of stable isotope transport

The interest of HDO and $H_2^{18}O$ in hydrology is due to their properties acting as tracers for water movements both in the liquid and vapour phases. The time evolution of isotope concentration profiles was first studied and modelled for free-water evaporating surfaces (Craig and Gordon, 1965). Zimmermann et al. (1967) showed that this model could be applied to saturated evaporating soils under steady-state conditions. This work was extended to non-saturated soils by Barnes and Allison (1983) for isothermal and steady-state conditions. Barnes and Allison (1984) considered non-isothermal conditions, where soil temperature was a prescribed function of depth, and they proposed corresponding analytical solutions. However, in order to understand, to describe, and/or to predict the evolution of isotope concentration profiles under evaporation for field conditions, a model able to describe both non-steady state and the time evolution of the atmospheric forcing is required. A first approach was proposed by Shurbaji and Phillips (1995) based on a modelling of coupled heat and water movement within the soil using the formalism of Philip and De Vries (1957). However, the upper boundary conditions had to be specified by

measurements of soil surface temperature and humidity. Since these data are seldom available, there is a need for a model fully interacting with the atmosphere, i.e. able to solve the surface energy budget. A simplified approach towards that direction was proposed by Mathieu and Bariac (1996) under constant potential evaporation and prescribed soil temperature profiles. Mélayah et al. (1996) generalised the approach to variable climatic conditions, as encountered under field situations, and to fully coupled heat and water transport. The theoretical basis of the bare soil heat and water transport model used in this study are very closed to that of Mélayah et al. (1996). The development of the isotope transport module also borrowed lots of the concept described in that early paper. However, some hypotheses were reconsidered and some inconsistencies corrected. We also revisited the specification of the resistance to isotope transport between the soil surface and the atmosphere, via the formulation of the kinetic fractionation factor. Sensitivity to this formulation is discussed in detail in the paper. The rationale beyond our study was to reconsider these early works by taking into account future extension of the modelling including (i) a better representation of the interactions between the soil and the atmosphere, (ii) the inclusion of vegetation and (iii) the identification of the strengths and weaknesses of current approaches encountered in the literature in order to design future laboratory and field experiments dedicated to process studies and to the validation of the SiSPAT-Isotope model.

3. The SiSPAT SVAT model

A model able to simulate heat, water and isotope species transfer within soils was developed. It was built from an existing 1D, mechanistic SVAT model called SiSPAT (Simple Soil Plant Atmosphere Transfer) (Braud et al., 1995; Braud, 2000, 2002). This model is forced by climatic data (air temperature and humidity, wind speed, incoming solar and longwave radiation and rainfall) measured at a reference height of typically 2 m above the vegetation with a time step of 15–30 min to 1 h and linearly interpolated at the time step of the model. Coupled heat and water transfer equations within the soil, including a sink term for root extraction and liquid and vapour transfer, are solved. Soil temperature and water matric potential are the independent prognostic variables. The upper boundary conditions of the soil module are provided by the solution of a set of five equations linking the atmosphere and the surface (energy budget over bare soil and vegetation, respectively, continuity of heat and water vapour transfer fluxes within the canopy, continuity of mass transfer at the soil surface). This SVAT model was extensively tested and validated against various data sets covering contrasted climatic and moisture conditions (e.g. Boulet et al., 1997; Braud et al., 1995, 1997; Calvet et al., 1999; Gonzalez-Sosa et al., 1999, 2001; Olioso et al., 2002). However, the partition between evaporation from soil and transpiration by plants was not properly validated, because only total evapotranspiration measurements were available. The use of stable isotope concentrations within soils could help filling this gap, but this required the adjunction of an isotope transfer module to the SiSPAT model. We describe below the bare soil version of this module. Details of the SiSPAT model formulation and numerical discretisation can be found in Braud (2000, 2002). Appendix B summarises the main equations for heat and water transport solved by the model for bare soil. Notations are defined in Appendix A.

4. Isotope transport equation

4.1. Definition of the concentration of an isotopic species

Natural stable water isotopes can move within a soil in the vapour and liquid phases. Therefore, the concentration of one isotopic species must be considered in both phases. The definition of the concentration of the isotopic species given below can be applied both to the liquid and the vapour phases. The concentration C_i (kg m^{-3}) of isotope i, namely HDO and $H_2^{18}O$ can be defined as

$$C_i = \frac{m_i}{V} \tag{1}$$

where m_i (kg) is the mass of isotope i, either in the liquid or in the vapour phase, and V (m^3) is the corresponding volume of water. Eq. (1) can be

rewritten as

$$C_i = \frac{m_i}{m_T}\frac{m_T}{V} \quad (2)$$

where m_T (kg) is the total mass of water (including the isotope species and ordinary water). The mass of a species is the product of the number of moles (N_i and N_w (mol) for isotopes and ordinary water, respectively) by the molar mass (see Appendix C) of these species (M_i and M_w (kg) for isotopes and ordinary water, respectively). Eq. (2) can therefore be expressed as:

$$C_i = \frac{N_i M_i}{N_i M_i + N_w M_w}\frac{N_i M_i + N_w M_w}{V} \quad (3)$$

Assuming that the water volumetric mass is independent of its isotopic concentration, i.e. that $N_i M_i \ll N_w M_w$ (Ménache, 1966), Eq. (3) can be approximated by

$$C_i = \frac{M_i}{M_w} R_i \rho \quad (4)$$

where $R_i = N_i/N_w$ (–) is the isotopic ratio of species i and ρ (kg m^{-3}) is the volumetric mass of water either in the liquid, ρ_w, or in the water vapour, ρ_v, phase.

4.2. Expression of isotopic concentration in delta notation

Although numerical computations were performed using the concentration defined above as the prognostic variable, results will be presented in delta notation (‰), classically defined as follows

$$\delta_i = \frac{R_i - R_{ref}}{R_{ref}} 1000 \quad (5)$$

where R_{ref} is a reference value given by the Vienna Standard Mean Ocean Water (V-SMOW) (see Appendix C). R_i can be deduced from the concentration by inverting Eq. (4):

$$R_i = \frac{M_w}{M_i}\frac{C_i}{\rho} \quad (6)$$

The use of the delta notation in ‰ is classical in isotope science leading to more tractable numbers.

4.3. Mass conservation equation for one isotopic species

The mass conservation equation for isotope i is expressed as

$$\frac{\partial(C_i^l \theta_l + C_i^v \theta_v)}{\partial t} = -\frac{\partial}{\partial z}[q_i] \quad (7)$$

where t is the time (s), z (m) is the depth within the soil, positively oriented downward with the origin at the soil surface, C_i^l (kg m^{-3}) (respectively, C_i^v (kg m^{-3})) is the concentration of isotope i in the liquid (respectively, vapour) phase, θ_l (m^3 m^{-3}) (respectively, θ_v (m^3 m^{-3})) is the volumetric liquid (respectively, vapour) content, and q_i (kg m^{-2} s^{-1}) is the total mass flux of isotope i. Note that $\theta_v = n_{soil} - \theta_l$, where n_{soil} (–) is the soil porosity.

The total flux is the sum of the isotope flux in the liquid phase, q_i^l (kg m^{-2} s^{-1}) and the vapour phase, q_i^v (kg m^{-2} s^{-1}). Both include a convection and a diffusion term, the latter being expressed by the Fick law. They are written, respectively, as follows

$$q_i^l = C_i^l q_l - D_i^{l^*}\frac{\partial C_i^l}{\partial z} \quad (8)$$

$$q_i^v = C_i^v q_v - D_i^{v^*}\frac{\partial C_i^v}{\partial z} \quad (9)$$

where q_l (m s^{-1}) (respectively, q_v (m s^{-1})) is the liquid (respectively, vapour) water flux, $D_i^{l^*}$ (respectively, $D_i^{v^*}$) is the total liquid (respectively, vapour) diffusivity (m^2 s^{-1}) for isotope i. The total liquid diffusivity can be expressed as (Mélayah et al., 1996)

$$D_i^{l^*} = D_i^{lo}\tau\theta_l + \Lambda|q_l| \quad (10)$$

where τ is the soil tortuosity (–), Λ (m) is the dispersivity length and D_i^{lo} (m^2 s^{-1}) is the molecular diffusivity of isotope i in liquid water (see Appendix C). In the simulations presented in this paper, Λ was set equal to zero, in order to be consistent with the studies used as reference for the evaluation of our model. Furthermore, under evaporation, convective and hydrodynamic dispersion processes are negligible as compared to the diffusion ones (Auriault and Adler, 1995).

Following Mélayah et al. (1996), the total vapour diffusivity is expressed as

$$D_i^{v^*} = (n_{soil} - \theta_l)\tau D_v \left(\frac{D_i^v}{D_v}\right)^{n_D} \quad (11)$$

where D_v (respectively, D_i^v) ($m^2\ s^{-1}$) is the vapour diffusivity of water (respectively, isotope) in air (see Appendix C). In most of the literature (e.g. Barnes and Allison, 1983, 1984; Mathieu and Bariac, 1996), the value $n_D = 1$ was used for the exponent. Mélayah et al. (1996) proposed the following relationship

$$n_D = 0.67 + 0.33 \exp\left(1 - \frac{\theta_l}{\theta_r}\right) \quad (12)$$

where θ_r ($m^3\ m^{-3}$) is the residual water content. Mélayah et al. (1996) used the results of Merlivat (1978a) to justify this expression. However, Merlivat's measurements were made in the atmosphere and it is not obvious to know if the formula can be extended to water vapour in soils. Furthermore, according to Brutsaert (1982), the exponent n_D depends on the air water content of the atmosphere and varies between 0.5 (turbulent flow), 2/3 (laminar flow), and 1 (molecular diffusion).

4.4. Relationship between liquid and vapour isotope concentration

The mass conservation equation for isotopic species provides one equation with two unknowns: namely, the liquid and vapour concentration. In order to be able to solve the equation, an additional relationship must be provided. Assuming instantaneous equilibrium between the liquid and vapour phases, the relationship between the corresponding liquid and vapour isotopic ratios can be written as (Mathieu and Bariac, 1996; Mélayah et al., 1996)

$$R_i^v = \alpha_i^* R_i^l \quad (13)$$

where α_i^* (–) is the liquid–vapour isotopic fractionation factor at equilibrium given by Majoube (1971) as a function of temperature T (K) (see Appendix C).

In terms of concentrations, insertion of Eq. (6) into Eq. (13) leads to

$$C_i^v = \frac{M_i}{M_w} R_i^v \rho_v = \frac{M_i}{M_w} \alpha_i^* R_i^l \rho_v = \alpha_i^* \frac{\rho_v}{\rho_w} C_i^l = \beta_i^* C_i^l \quad (14)$$

with

$$\beta_i^* = \alpha_i^* \frac{\rho_v}{\rho_w} \quad (15)$$

4.5. Final conservation equation to be solved

Introducing Eqs. (8), (9) and (14) into the mass conservation equation (Eq. (7)), leads to the following development

$$\frac{\partial\{[\theta_l + (n_{soil} - \theta_l)\beta_i^*]C_i^l\}}{\partial t} = -\frac{\partial}{\partial z}[q_i^l + q_i^v] \quad (16)$$

$$\frac{\partial\{[\theta_l + (n_{soil} - \theta_l)\beta_i^*]C_i^l\}}{\partial t} = -\frac{\partial}{\partial z}\left[C_i^l q_l - D_i^{l^*}\frac{\partial C_i^l}{\partial z} + \beta_i^* q_v C_i^l - D_i^{v^*}\frac{\partial \beta_i^* C_i^l}{\partial z}\right] \quad (17)$$

$$\frac{\partial\{[\theta_l + (n_{soil} - \theta_l)\beta_i^*]C_i^l\}}{\partial t} = -\frac{\partial}{\partial z}\left[\left(q_l + \beta_i^* q_v - D_i^{v^*}\frac{\partial \beta_i^*}{\partial z}\right)C_i^l - (D_i^{l^*} + D_i^{v^*}\beta_i^*)\frac{\partial C_i^l}{\partial z}\right] \quad (18)$$

$$\frac{\partial[\Theta_i C_i^l]}{\partial t} = \frac{\partial}{\partial z}\left[D_i^{lv^*}\frac{\partial C_i^l}{\partial z} - Q_i^{lv^*} C_i^l\right] \quad (19)$$

with

$$\Theta_i = [\theta_l + (n_{soil} - \theta_l)\beta_i^*] \quad (20)$$

$$Q_i^{lv^*} = \left(q_l + \beta_i^* q_v - D_i^{v^*}\frac{\partial \beta_i^*}{\partial z}\right) \quad (21)$$

$$D_i^{lv^*} = (D_i^{l^*} + D_i^{v^*}\beta_i^*) \quad (22)$$

Eq. (19) is a non-linear partial derivative equation with the same form as the classical convection–dispersion equation for solute transport. It can completely be solved for any species i, once initial and boundary conditions are provided. Eq. (19) is very close to Eq. (44) of Mélayah et al. (1996). However, we identified some inconsistencies in their derivations. Consequently, the discretisation we implemented

(see Appendix D) was directly derived from Eq. (19) and is therefore not prone to the same misprints.

5. Boundary conditions and formulation of the resistance to isotope transport between the soil surface and the atmosphere

5.1. Boundary conditions

The upper and lower boundary conditions can be either a known value of the liquid isotopic concentration or a known flux. In Section 5.2, we describe in more details how the surface isotopic flux can be calculated as a function of atmospheric conditions and atmospheric isotopic concentration.

The surface isotopic flux E_i (kg m^{-2} s^{-1}) is assumed to be proportional to the gradient of isotopic concentration between the atmosphere C^{v}_{ia} (kg m^{-3}) (considered at a reference level z_a where climatic data and atmospheric vapour isotopic concentration are assumed to be measured) and the soil surface C^{v}_{is} (kg m^{-3})

$$E_i = \frac{C^{v}_{is} - C^{v}_{ia}}{r_i} \tag{23}$$

where r_i (s m^{-1}) is the resistance to isotopic species transport. Following the notations proposed by Barnes and Allison (1983), r_i can be written

$$r_i = r_a \alpha_{iK} \tag{24}$$

where r_a (s m^{-1}) is the aerodynamic resistance to heat and water vapour transfer and $\alpha_{\tau K}$ (–) is the so-called isotopic kinetic fractionation factor.

The isotopic vapour concentration at the surface and in the atmosphere can be written (see Eq. (4)) as functions of the corresponding isotopic ratio R^{v}_{is} and R^{v}_{ia}, the specific humidity q_s and q_a (kg kg^{-1}) at the soil surface and in the atmosphere, respectively, and the air volumetric mass ρ_a (kg m^{-3}). This leads to:

$$E_i = \frac{\rho_a}{\alpha_{iK} r_a} \frac{M_i}{M_w} (R^{v}_{is} q_s - R^{v}_{ia} q_a) \tag{25}$$

Finally, the use of Eq. (13) allows to relate E_i to the liquid isotopic concentration R^{l}_{is} at the soil surface calculated by the solution of Eq. (19)

$$E_i = \frac{\rho_a}{\alpha_{iK} r_a} \frac{M_i}{M_w} (\alpha^*_i R^{l}_{is} q_s - R^{v}_{ia} q_a) \tag{26}$$

In this final expression it is assumed that the liquid fraction is in equilibrium with the overlying vapour.

5.2. Formulations of the resistance to isotope transfer between the soil surface and the atmosphere

Various expressions are available in the literature for the kinetic fractionation factor according to hypotheses made on the influence of molecular and turbulent diffusion, respectively. It is assumed that turbulent diffusion does not produce any isotopic fractionation, whereas molecular diffusion does (Craig and Gordon, 1965).

Mathieu and Bariac (1996) reported a general formulation proposed by Merlivat and Jouzel (1978) of the kinetic fractionation factor related to the turbulent, r_{aT}, and molecular, r_{am}, resistances to water vapour transfer:

$$\alpha_{iK} = \frac{\left[\left(\frac{D_v}{D^{v}_i}\right)^{n_K} + \frac{r_{aT}}{r_{am}}\right]}{1 + \frac{r_{aT}}{r_{am}}} \tag{27}$$

Introducing

$$\varepsilon_{iK} = \frac{D_v}{D^{v}_i} - 1 \ll 1,$$

and noting that $r_a = r_{aT} + r_{am}$, Eq. (27) can be simplified as (Merlivat and Coantic, 1975):

$$\alpha_{iK} = 1 + n_K \left(\frac{D_v}{D^{v}_i} - 1\right) \frac{r_{am}}{r_a} \tag{28}$$

Brutsaert (1982) proposed formula for the molecular diffusion for smooth and rough surfaces. These formulae were validated by Merlivat and Coantic (1975) and Merlivat (1978b) using stable isotope of water evaporating surfaces. These formulae read

$$\begin{cases} r_{am} = 13.6\left(\frac{\nu}{D_v}\right)^{n_K} & \text{for } \left(\frac{u^* z_{om}}{\nu}\right) \le 1 \\ & \text{and with } n_K = 2/3 \\ r_{am} = 7.3\left(\frac{u^* z_{om}}{\nu}\right)^{1/4}\left(\frac{\nu}{D_v}\right)^{n_K} & \text{for } \left(\frac{u^* z_{om}}{\nu}\right) \ge 1 \\ & \text{and with } n_K = 1/2 \end{cases} \tag{29}$$

for smooth (laminar) and rough (turbulent) surfaces, respectively. In Eq. (29), u^* (m s^{-1}) is the friction velocity, z_{om} (m) is the roughness length for

momentum, ν ($m^2\ s^{-1}$) is the air kinematic viscosity. Brutsaert (1982) derived these formulae from wind tunnel experiments. To our knowledge, nobody tried to verify if they were still valid for field or natural conditions.

An alternative approach proposed by Stewart (1975) and cited by Mathieu and Bariac (1996) simplifies Eq. (27) and combines the influence of turbulent and molecular resistances into a modified exponent $n_K{}'$, determined empirically, leading to:

$$\alpha_{iK} = \left(\frac{D_v}{D_i^v}\right)^{n'_K} \tag{30}$$

Mathieu and Bariac (1996) proposed the following expression for the exponent

$$n'_K = \frac{(\theta_s - \theta_r)n_a + (\theta_{sat} - \theta_s)n_s}{(\theta_{sat} - \theta_r)} \tag{31}$$

where θ_s is the soil surface volumetric water content and θ_{sat} is the saturated water content. The authors used $n_a = 0.5$ and $n_s = 1$ leading to a value $n_K{}' = 0.5$ for a saturated soil and $n_K{}' = 1$ for a dry soil.

When molecular diffusion is neglected, as in Mélayah et al. (1996), resistances to water vapour and isotope vapour are identical, i.e.

$$\alpha_{iK} = 1 \tag{32}$$

Note, however, that Mélayah et al. (1996) introduced an exponent non-equal to one for the definition of the isotopic water vapour diffusivity into the soil (see Eqs. (11) and (12)), which might partly compensate the value of one used for the kinetic fractionation factor.

When only molecular diffusion is considered (see Barnes and Allison, 1983 for instance), the kinetic fractionation factor reads:

$$\alpha_{iK} = \left(\frac{D_v}{D_i^v}\right) \tag{33}$$

As no agreement exists on which formula to employ and in which conditions, we tested formulations (28), (30), (32) and (33) in the model. Sensitivity tests to these expressions are provided in Section 6 and a summary of the various formulae is given in Tables 4 and 6. Note that in this study, we used the values of the ratio D_v/D_i^v proposed by Merlivat (1978a) (see Appendix C). Recently, Cappa et al. (2003) proposed new values for these ratio. They have not been used in the present study, but will be tested in future work.

5.3. Numerical solution and discretisation

The numerical discretisation of the isotope transport equation is presented in Appendix D. The reader can refer to Braud (2000, 2002) for details on the numerical solution of the heat and water transport equations.

First sensitivity tests showed that the numerical solution of the isotopic species transport equation was very sensitive to the accuracy of the heat and water transport equation solution. Improvements of the numerical solution of the SiSPAT model, presented by Braud (2002), had to be implemented in order to reach this accuracy. The use of the classical form of the Richards equation (see Appendix B) can lead to large mass conservation errors when the soil is near saturation, due to the capillary capacity approaching zero. As shown by Celia et al. (1990), this problem can be overcome by using an iterative solution for the heat and water transport equation and by introducing a corrective factor depending on the water content to ensure mass conservation.

Mathieu and Bariac (1996) proposed some likelihood tests for a numerical model of isotopic species transport (see Section 6). When trying to simulate those examples, especially Test (1), instability in the solution was found. The source of these instabilities lied once again in the numerical solution of the heat and water transfer equation. Haverkamp et al. (1977) and Vauclin et al. (1979) showed that the use of geometric means to estimate the transport coefficients at the inter-nodes were leading to more accurate solutions of the infiltration equation, especially near the infiltration front. This weighing scheme was originally implemented in SiSPAT (Braud, 2000). However, we found inaccurate results in case of steady state evaporation, with a non-constant evaporation rate along the vertical profile, although top and bottom fluxes were identical. This non-constant flux profile was responsible for instabilities in the isotopic concentration profiles. The use of arithmetic means instead of geometric ones in the interpolation of transport coefficients of the heat and water transfer equation successfully solved the problem.

Eventually, it must be underlined that the solution of the isotopic species transport equation requires a high resolution of the vertical profile close to the surface, especially to capture the vapour return (see Section 6), with inter-nodes spacing of the order of 10^{-6}–10^{-4} m near the soil surface, whereas a value of 10^{-3} m was sufficient to get stable results with the heat and water transfer model. A time step of less than 50 s was used, but its value (automatically calculated by the model) can be much smaller, depending on the rate of change in the calculated variables.

6. Verification of the numerical solution

6.1. Likelihood tests

In order to verify that the orders of magnitude and the processes were correctly taken into account by the model, we performed six likelihood tests proposed by Mathieu and Bariac (1996).

We considered a soil column, 1 m deep, the soil having the properties of the Yolo Light clay (Philip, 1957). The retention and hydraulic conductivity curves were described by the Van Genuchten (1980) and Brooks and Corey (1964) closed-form equations, respectively

$$\frac{\theta_l - \theta_r}{\theta_{sat} - \theta_r} = \left[1 + \left(\frac{h}{h_g}\right)^n\right]^{-m} \tag{34}$$

with (Burdine, 1953)

$$n = \frac{2}{1-m} \tag{35}$$

$$K(\theta) = K_{sat}\left(\frac{\theta_l}{\theta_{sat}}\right)^{\eta} \tag{36}$$

where h (m) is the soil water pressure head. Parameter values were taken from the Grizzly data base (Haverkamp et al., 1998) and they are given in Table 1.

We considered isothermal conditions with an arbitrary soil temperature of $T=303$ K. The soil was supposed to be initially saturated, with an hydrostatic soil water pressure profile. The initial isotopic composition of the soil water, $\delta^{l}_{i\_alim}$, was assumed to be uniform and is referred to as 'alimentation water'. At the bottom of the column, we used a zero flux condition for water and isotope fluxes. At the soil surface, instead of solving the energy budget, we used a simplified boundary condition by considering constant value for the potential evaporation ($E_p = 1.005\times10^{-5}$ kg m^{-2} s^{-1}), the actual surface evaporation flux being parameterised according to the approach of Mathieu and Bariac (1996)

Table 1
Parameters of the retention and hydraulic conductivity curves described by the van Genuchten and Brooks and Corey expressions, respectively

Parameter	Value
Saturated water content, θ_{sat}	0.35 m^3 m^{-3}
Residual water content, θ_r	0.01 m^3 m^{-3}
Shape parameter of the retention curve, n	2.22
Shape parameter of the retention curve, m	0.099
Scale value of the water pressure, h_g	−0.193 m
Saturated hydraulic conductivity, K_{sat}	1.23×10^{-7} m s^{-1}
Shape parameter of the conductivity curve, η	9.14

See Eqs. (34)–(36).

$$E = E_p \frac{h_s - h'_a}{1 - h'_a} \tag{37}$$

where h_a (–) (respectively, h_s) is the air (respectively, soil surface) relative humidity and $h_a{}'$ is given by

$$h'_a = h_a \frac{\rho^v_{sat}(T_a)}{\rho^v_{sat}(T_s)} \tag{38}$$

where T_a (K) (respectively, T_s) is the air (respectively, the soil surface) temperature and $\rho^v_{sat}(T)$ is the saturated volumetric mass of water vapour (kg m^{-3}). We used values of $T_a=303$ K (the same value as in the soil) and $h_a=0.2$.

With this formulation of the surface evaporation flux, the corresponding surface isotopic flux can be written

$$E_i = \frac{E_p}{\alpha_{iK}} \frac{M_i}{M_w} \frac{\alpha^*_i R^l_{is} h_s - h'_a R^v_{ia}}{1 - h'_a} \tag{39}$$

and provides the upper boundary condition for the isotope transport module, once a value of the atmospheric isotopic ratio has been chosen.

For these tests, we used Eq. (30) with an exponent given by Eq. (31). The main characteristics of the six likelihood tests are summarised in Table 2.

Table 2
Main characteristics and results of the likelihood tests performed with the SiSPAT-Isotope model

Test	Parameters					Results				
	α_i^*	D_i^v	D_i^l	α_{iK}	δ_a^v	(a)	(b)	(c)	(d)	Comments
(1)	1	D^v	0	1	δ_{alim}	0	0	–	–	No change $\delta(z,t)=\delta_{alim}$
(2)	1	D^v	0	1	δ_a^v	−6.3	−42.5	6.7		Surface impoverishment towards δ_a^v
(3)	α_i^*	D^v	0	1	$\delta_{a\ lim}$	+8.8	+68.6	–	7.7	Surface enrichment without vapour return
(4)	α_i^*	D^v	0	1	δ_a^v	+6.7	+52.4	7.1	7.6	Surface enrichment with vapour return
(5)	α_i^*	D^v	D_i^l	1	δ_a^v	+5.5	+43.3	6.7	7.8	Thicker peak than Test (4)
(6)	α_i^*	D_i^v	D_i^l	α_{iK}	δ_a^v	+10.0	+56.3	2.0	2.7	Larger and thicker peak than Test (5)

$\delta^l_{D\_alim}=-65$ (‰), $\delta^l_{O\_alim}=-8$ (‰), and $\delta^v_{D\_a}=-112$ (‰), $\delta^v_{O\_a}=-15$(‰). (a) Maximum isotopic enrichment as compared to the alimentation water for $H_2^{18}O$, in δ notations. (b) Maximum isotopic enrichment as compared to the alimentation water for HDO, in δ notations. (c) Slope of the HDO/$H_2^{18}O$ relationship in the vapour phase. (d) Slope of the HDO/$H_2^{18}O$ relationship in the liquid phase.

Four parameters were considered for the analysis: the equilibrium isotopic fractionation factor, α_i^*, the isotopic water vapour diffusivity, D_i^v, the isotopic liquid diffusivity, D_i^l and the atmospheric vapour isotopic ratio in delta notation, δ_{ia}^v. Results after a 250-day simulation period, ensuring that a steady state was reached, are provided in Fig. 1 for HDO and $H_2^{18}O$. They are also summarised in the right-hand side of Table 2.

- Test (1) allowed to check the stability of the numerical scheme. In this test, equilibrium and

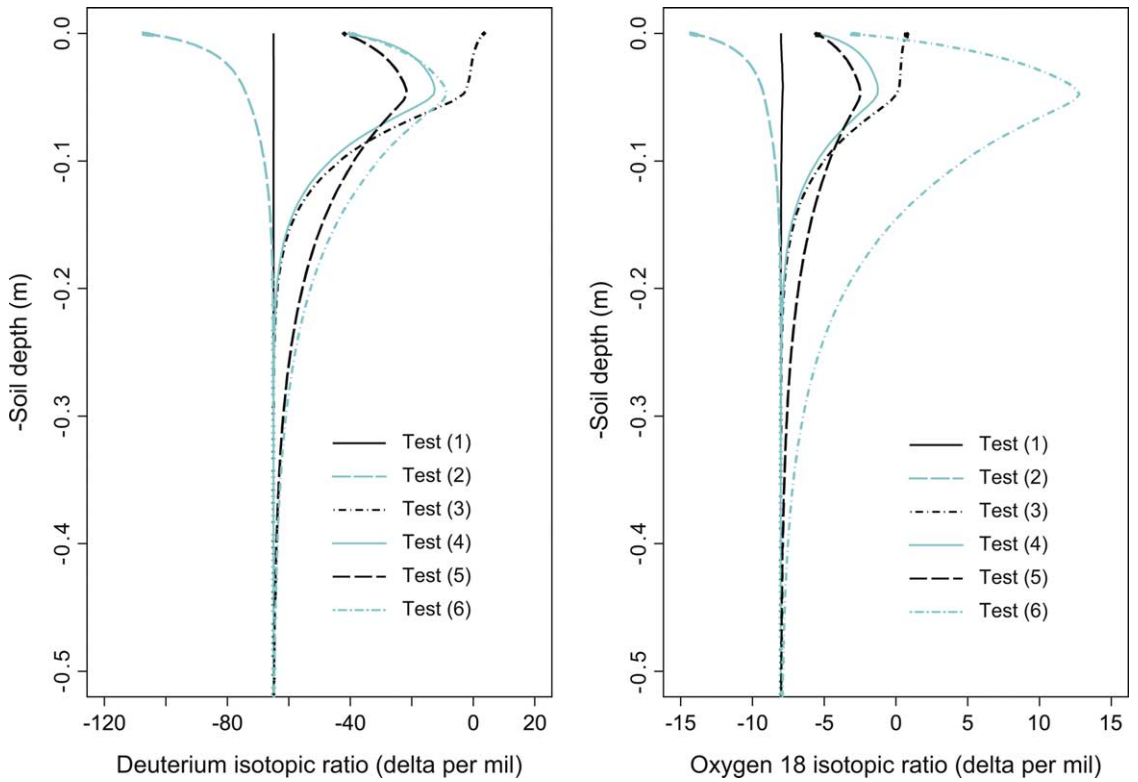

Fig. 1. Simulated deuterium and oxygen 18 concentration profiles for the six likelihood tests. Simulations were conducted using a 1 m depth soil column, but results are presented for the first 50 cm only.

kinetic isotopic fractionation factors were neutralised and liquid diffusion was not allowed. Water vapour diffusivity was also taken equal to that of ordinary water. The expected theoretical solution was therefore uniform isotope concentration profiles. This result was effectively obtained by the model, with a deviation of less than 0.1 δ (Fig. 1). The numerical solution was obtained with a top layer thickness of the order of 10^{-6} m. With a value of about 10^{-3} m, the deviation from the expected constant profile could reach 2.5 δ. These figures must be compared to the accuracy of the isotope concentration measurement which is ± 0.15 δ for $H_2^{18}O$ and ± 0.5 δ for deuterium. This test was the most severe for the model due to the steady state conditions and the small values of the fluxes, explaining the very fine spatial discretisation required to get accurate results.

- Test (2) was equivalent to Test (1), except that a realistic value (i.e. much lower than the alimentation water) was given to the air vapour isotopic ratio. This test showed the consistency of the surface flux calculation. As long as evaporation proceeds and the soil column dries out, the isotopic concentration of the liquid is expected to tend towards the value of the atmospheric vapour. After 250 days, the surface concentration was -107.5 δ for deuterium (respectively, -14.3 δ for $H_2^{18}O$) whereas the expected value (i.e. the value of the air water vapour concentration) was -112 δ for deuterium (respectively, -15 δ for $H_2^{18}O$). The slope of the HDO/$H_2^{18}O$ relationship was equal to 6.7, corresponding to the expected value given by

$$\frac{\delta^{l}_{D\_alim} - \delta^{v}_{D\_a}}{\delta^{l}_{O\_alim} - \delta^{v}_{O\_a}}$$

for our case study.

- In Test (3), the equilibrium isotopic fractionation factor was considered (see Eq. (C.4)), with still the liquid and vapour diffusivities equal to zero and to that of ordinary water, respectively. However, the atmosphere isotopic concentration was equal to that of the alimentation water. A surface enrichment was simulated, without vapour return, which was expected because air water vapour influence was inhibited.
- Test (4) was similar to Test (3) but a realistic value (i.e. much lower than the alimentation water) was given to the air vapour isotopic ratio. Test (4) showed that, when the influence of air water vapour was reintroduced, the expected vapour return was simulated.
- In Test (5), liquid diffusion influence was reintroduced, leading to a thicker but smaller enrichment peak than simulated in Test (4), due to diffusion.
- Finally, kinetic fractionation influence was reintroduced in Test (6), and the isotope water vapour diffusivity was set equal to its true value. The results led to a higher and thicker peak than the one obtained in all the previous cases.

As also mentioned by Mathieu and Bariac (1996), the slope of the simulated HDO/$H_2^{18}O$ relationship exhibited values around 8 for Tests (3)–(5), as expected in the liquid phase, when only equilibrium fractionation was considered. In Test (6), the slope value decreased to a value around 3 for the liquid phase, showing the signature of the kinetic fractionation factor influence.

6.2. Comparison with the analytical solution of Barnes and Allison (1983)—saturated case

Following Zimmermann et al. (1967), Barnes and Allison (1983) (BA83 below) gave the analytical solution of isotopic transport for a saturated soil column, evaporating into an atmosphere of constant humidity, h_a, and isotopic composition, δ^{v}_{ia}, under isothermal conditions. The soil column was assumed to be constantly re-alimented with water of isotopic ratio $\delta^{l}_{i\_alim}$, so that the water flux within the column was constant and equal to the evaporation rate E (kg m^{-2} s^{-1}) given by Eq. (37). When steady state was reached, there was equilibrium between the diffusive and the convective fluxes of isotopic species (BA83). The isotopic concentration is then given by

$$\delta^{l}_{i}(z,t) = \delta^{l}_{i\_alim} + (\delta^{l}_{is} - \delta^{l}_{i\_alim})\exp\left(-\frac{E}{D^{l^*}_{i}}z\right) \quad (40)$$

where the surface value of the isotopic concentration, δ^{l}_{is}, was given by BA83 with $n_K = 1$ in Eq. (33)

(only molecular diffusion was considered by BA83):

$$\alpha_i^*(1+\delta_{is}^{l}) = [(1-h_a)\alpha_{iK}(1+\delta_{i\_alim}^{l}) + h_a(1+\delta_{ia}^{v})] \quad (41)$$

Note that BA83 assumed the following definition for the isotopic concentration

$$C_i^{l} = \rho_w R_i^{l} \quad (42)$$

which is different from Eq. (4) we used in our method. However, it appeared that the use of Eq. (4) did not change the calculated concentration profiles. Only the surface fluxes were modified, i.e. multiplied by a factor M_i/M_w as compared to the use of Eq. (42). In the following, results were therefore obtained using Eq. (42) for the isotope concentration definition.

Consistency of the model under saturated conditions was tested using the properties of the Yolo Light Clay soil given in Section 6.1. Parameters of the simulation are given in Table 3. A 1 m deep soil column was considered under isothermal conditions ($T=T_a=303$ K). The soil water pressure was assumed to be hydrostatic at the beginning of the simulation. The lower boundary condition was a constant water pressure equal to its initial value ($h=1$ m). This choice allowed permanent water supply at the bottom of the soil column and conservation of saturation. Numerically, however, a small fraction of the soil (0–0.075 m) was not fully saturated, with a maximum deviation of 0.005 $m^3\,m^{-3}$ from saturation. After 250 days of simulation, a duration long enough to reach steady state, the numerical results were compared with the BA83 solution (see Eqs. (40) and (41))). The results presented in Table 3 show a very good agreement between the model and the BA83 analytical solution for both HDO and $H_2^{18}O$.

Fig. 2 and Table 4 show the sensitivity of the solution to different formulations of the kinetic fractionation factor. This sensitivity is large, especially for $H_2^{18}O$ concentration. The value $\alpha_{iK}=1$ (Mélayah et al., 1996) leads to a slope of the relationship HDO/$H_2^{18}O$ of about 8.5, a value consistent with an equilibrium process ($h_s=100\%$) and inconsistent with the classical decrease in the slope observed experimentally for evaporating surfaces taking account of a kinetic effect (e.g. Gat, 1981; Gonfiantini, 1986). The formulation of Mathieu and Bariac (1996) (with $\alpha_{iK}=(D_v/D_i^v)^{n'_K}$ and $n_K{}'$ for a saturated soil) leads to a smaller surface enrichment and a higher slope than that obtained using the 'molecular diffusion only' hypothesis. The values obtained by the Brutsaert (1982) model are very close to that of the $\alpha_{iK}=1$ hypothesis. Although the kinetic fractionation factor evolves in time in the Brutsaert (1982) formulation, we can assume that the right-hand side term of Eq. (28) is negligible, which is very consistent with a high value for the aerodynamic resistance (around 2500 s m^{-1})[1]. Note also that this formula is the only one requiring the specification of

Table 3
Parameters values and model/theoretical results in a case of isothermal saturated soil

Parameters	Values
Steady state evaporation rate	$E=1.003\times10^{-5}$ kg m^{-2} s^{-1}
Saturated water content	$\theta_{sat}=0.35$ m^3 m^{-3}
Soil tortuosity	$\tau=0.67$
Air temperature	$T_a=303$ K
Air relative humidity	$h_a=0.2$
Initial and alimentation HDO concentration	$\delta^{l}_{D\_alim}=0$ (‰)
Atmospheric water vapour HDO concentration	$\delta^{vl}_{Da}=-100$ (‰)
Initial and alimentation $H_2^{18}O$ concentration	$\delta^{l}_{O\_alim}=0$ (‰)
Atmospheric water vapour $H_2^{18}O$ concentration	$\delta^{v}_{Oa}=-14$ (‰)

Results	Model results[a]	Theoretical results
Surface liquid HDO concentration	73.85	74.12
Surface liquid $H_2^{18}O$ concentration	29.06	29.15
Slope of the HDO/$H_2^{18}O$ relationship	2.54	2.55
HDO concentration profile	Confounded with theory	$\delta^{l}_{D}(z,t)=74.12\exp(-16.72z)$
$H_2^{18}O$ concentration profile		$\delta^{l}_{O}(z,t)=29.15\exp(-17.01z)$

[a] When Eq. (4) was used for the definition of isotope concentration the surface isotopic concentrations were 73.93 (‰) for HDO and 29.09 (‰) for $H_2^{18}O$.

[1] Note that when using Eq. (37) to derive the actual evaporation flux, E, an aerodynamic resistance can be recalculated by $r_a=\rho_a(q_s-q_a)/E$.

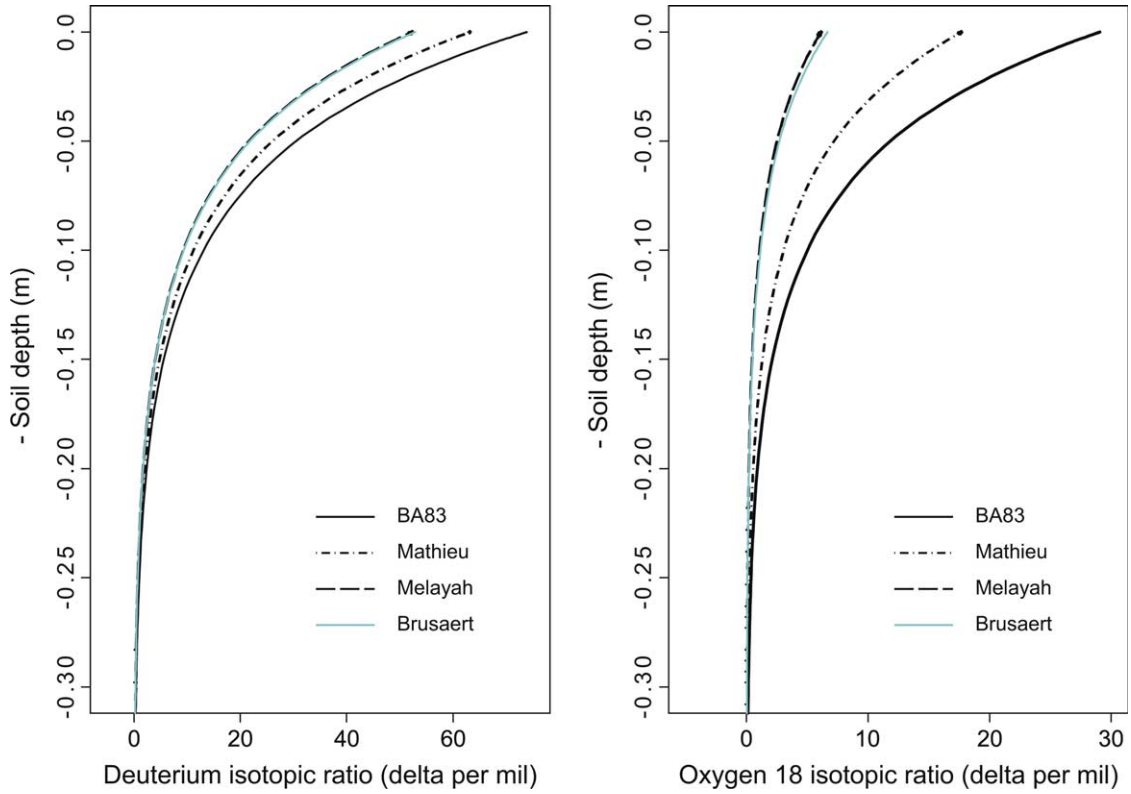

Fig. 2. Comparison of the steady state HDO (left) and $H_2^{18}O$ (right) concentration profiles for different formulation of the kinetic fractionation factor under saturated conditions. Simulations were conducted using a 1 m depth soil column, but results are presented for the first 30 cm only.

a wind speed and a roughness length for momentum value. It should therefore be more general under changing atmospheric conditions. However, it is difficult from this unique test to determine which formulation has to be retained.

6.3. Comparison with the analytical solution of Barnes and Allison (1984)—non-saturated case

Barnes and Allison (1984) (BA84) proposed an analytical solution for evaporation of an unsaturated

Table 4
Comparison of the simulated surface concentrations of HDO, δ_D^s, and $H_2^{18}O$, δ_O^s, for various formulations of the kinetic fractionation factor under saturated conditions

	$\alpha_{iK}=\left(\frac{D_v}{D_i^v}\right)$ Eq. (33); Barnes and Allison (1983)	$\alpha_{iK}=\left(\frac{D_v}{D_i^v}\right)^{n_K'}$ Eqs. (30) and (31); Mathieu and Bariac (1996)	$\alpha_{iK}=1$ Eq. (32); Mélayah et al. (1996)	$\alpha_{iK}=1+n_K\left(\frac{D_v}{D_{vi}}-1\right)\frac{r_{am}}{r_a}$ Eqs. (28) and (29); Brutsaert (1982)
Calculated δ_D^s	73.85	63.19	52.37	52.87
Theoretical δ_D^s	74.12	63.30	52.56	–
Calculated δ_O^s	29.06	17.67	6.13	6.66
Theoretical δ_O^s	29.15	17.58	6.13	–
Calculated HDO/$H_2^{18}O$ slope	2.54	3.58	8.54	7.94
Theoretical HDO/$H_2^{18}O$ slope	2.55	3.60	8.57	–

Theoretical values were calculated using Eq. (41) with the corresponding values of the kinetic fractionation factor. For the Mathieu and Bariac (1996) formulation, $n_K'=0.5$ for saturated conditions.

soil under non-isothermal conditions, once steady state conditions were reached. The soil column was assumed to be constantly supplied with water at the bottom. This solution was given by the differential equation (Eq. (29) of BA84)

$$\frac{d\delta_i^l}{dz} + (z_1 + h_u z_v)^{-1}(\delta_i^l - \delta_{i\_alim}^l) = h_u z_v (z_1 + h z_v)^{-1}(\alpha_{iK} - \alpha_i^*) \times \frac{d}{dz}[\mathrm{Ln}(h_u \rho_{vsat}(\alpha_{iK} - \alpha_i^*))] \quad (43)$$

where h_u (–) is the relative humidity at depth z, $n_K = 1$ in the expression of the kinetic fractionation factor (Eq. (31))

$$z_1 = \frac{D_i^{l^*}}{E} \quad (44)$$

and

$$z_v = \frac{D_i^{v^*} \rho_{vsat}}{\rho_w E} \quad (45)$$

Once the water and heat transfer equations are solved (see Appendix B), soil temperature T, water pressure head, h, and water content profiles, θ, are known. The saturated volumetric mass, ρ_{vsat}, can be calculated as a function of temperature, as well as the relative humidity, h_u, by using the Kelvin law

$$h_u = \exp\left(\frac{gh}{RT}\right) \quad (46)$$

where g (m s^{-2}) is the acceleration of gravity and $R = 461.5$ J kg^{-1} is the perfect gas mass constant for water vapour. The diffusion coefficients can be evaluated using Eqs. (10) and (11) with $\Lambda = 0$ and $n_K = 1$. Eq. (43) can then be solved using classical finite differences, once the surface concentration value is prescribed.

As in Section 6.2, we used Eq. (42) for the definition of concentration. In these simulations, the kinetic fractionation factor was calculated by Eq. (33).

Table 5 gives the parameters used in the numerical simulation. As an example, the comparison between the analytical and the numerical solution for a 1 m deep soil column of Yolo Light Clay is presented in Fig. 3 (left) for deuterium. The agreement is very fair, although the simulated value of the peak enrichment is slightly overestimated.

Table 5
Parameters values and model versus theoretical results in case of non-saturated, non-isothermal soil, with the exponential temperature profile proposed by Barnes and Allison (1984)

Parameter	Values
Potential evaporation	$E_p = 2.0\times10^{-4}$ kg m^{-2} s^{-1}
Steady state evaporation rate (250 days)	$E = 0.982\times10^{-5}$ kg m^{-2} s^{-1}
Saturated water content	$\theta_{sat} = 0.35$ m^3 m^{-3}
Soil temperature profile	$T(z) = 20(1 + \exp(-20z))$ (°C)
Soil tortuosity	$\tau = 0.67$
Air temperature	$T_a = 313$ K
Air relative humidity	$h_a = 0.2$
Initial and alimentation HDO concentration	$\delta^l_{D\_a\ lim} = 0$ (‰)
Atmospheric water vapour HDO concentration	$\delta^{vl}_{Da} = -100$ (‰)
Initial and alimentation $H_2^{18}O$ concentration	$\delta^l_{O\_a\ lim} = 0$ (‰)
Atmospheric water vapour ^{18}O concentration	$\delta^v_{Oa} = -14$ (‰)

Results	Model results	Theoretical results
Maximum liquid HDO concentration	39.62	37.22
Maximum liquid $H_2^{18}O$ concentration	19.92	19.52
Slope of the HDO/$H_2^{18}O$ relationship (liquid)	1.91	1.92
Slope of the HDO/$H_2^{18}O$ relationship (vapour)	3.06	3.07

In their paper, BA84 discussed the role of temperature gradients on the isotopic concentration. When mass transfer induced by temperature gradients are taken into account, the water vapour flux can be written as a function of the soil water pressure head and temperature

$$q_v = D_v \frac{\partial \rho_v}{\partial z} = D_v \frac{\partial \rho_v}{\partial h}\frac{\partial h}{\partial z} + \xi D_v \frac{\partial \rho_v}{\partial T}\frac{\partial T}{\partial z} \quad (47)$$

where ξ (–) is the temperature gradient enhancement factor (Philip and De Vries, 1957), accounting for increased transport due to differences between local and macroscopic temperature gradients. In their study, BA84 assumed $\xi = 1$. They claimed that if $\xi > 1$, their result would remain valid. However, it is probably not true, because in that case, the energy balance equation would lead to different equilibrium temperature

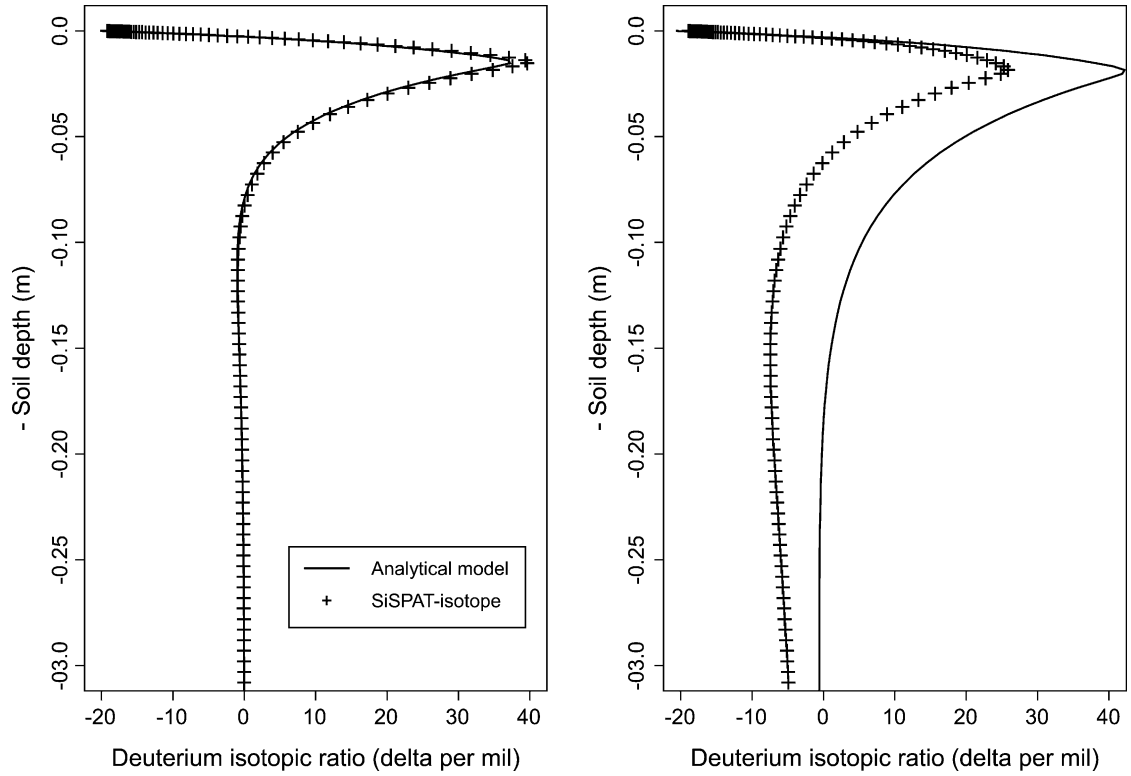

Fig. 3. Left: comparison between the analytical (full line) and numerical deuterium concentration profile (crosses) in case of a non-saturated, non-isothermal soil with the temperature gradient enhancement factor $\xi = 1$ (see Eq. (47)). Right: same as before with $\xi = 1.5$. Simulations were conducted using a 1 m depth soil column, but results are presented for the first 30 cm only.

profiles, modifying the equilibrium fractionation factor, relative humidity and saturated vapour volumetric mass. This is illustrated in Fig. 3 (right) for deuterium which compares the numerical profile (crosses) obtained with $\xi = 1.5$ and the analytical solution of Eq. (43) using the calculated soil temperature, water pressure and water content profiles. The difference between both could be the signature of the temperature gradient influence on the equilibrium and kinetic fractionation factor when the enhancement factor ξ is larger than one. Note that model results are consistent with what was expected: the non-isothermal profiles lead to an impoverishment below the peak, more important that when $\xi = 1$. Note also that in order to get reasonable values for the isotope concentration, we had to let the temperature profile equilibrate (leading to a final linear profile instead of the initial exponential one). Without this temperature equilibrium, the energy budget was not verified leading to numerical instabilities. Their influence was reduced in the BA84 case where $\xi = 1$. This result shows that under non-isothermal conditions, it is probably advisable to use fully coupled heat and water transport equations in order to avoid such numerical instabilities and errors in the calculated isotope concentrations.

Table 6 shows the sensitivity of the steady state profiles to five different formulations of the kinetic fractionation factor α_{iK}. Differences between all the formulations are much smaller in the non-saturated case than in the saturated one. Considering that the accuracy of the oxygen 18 concentration measurements is 0.1 δ, 0.5 δ for deuterium and that the depth of the peak can be determined with a precision of about 0.5 cm, Eqs. (30) and (33) lead to very close results. Results obtained by using Eqs. (29) and (32)

Table 6
Comparison of the simulated maximum concentrations of HDO, δ_D^{max}, and $H_2^{18}O$, δ_O^{max}, for various formulations of the kinetic fractionation factor under non-saturated, non-isothermal conditions

	$\alpha_{iK} = \left(\frac{D_v}{D_i^v}\right)$	$\alpha_{iK} = \left(\frac{D_v}{D_i^v}\right)^{n'_K}$	$\alpha_{iK} = 1$	$\alpha_{iK} = 1 + n_K\left(\frac{D_v}{D_{vi}} - 1\right)\frac{r_{amol}}{r_a}$	$\alpha_{iK} = 1$ and $n_D \neq 1$
	Eq. (33); Barnes and Allison (1983)	Eqs. (30) and (31) Mathieu and Bariac (1996)	Eq. (32); Mélayah et al. (1996)	Eqs. (28) and (29); Brutsaert (1982)	Eqs. (32) and (12); Mélayah et al. (1996)
	Case 1	Case 2	Case 3	Case 4	Case 5
Calculated δ_D^{max}	44.52	44.32	42.65	42.71	39.13
Calculated δ_O^{max}	22.1	21.93	19.93	20.00	16.01
Depth of the maximum (m)	0.0193	0.0193	0.0212	0.0212	0.0193
Calculated liquid HDO/$H_2^{18}O$ slope	2.00	2.01	2.12	2.11	2.41
Calculated vapour HDO /$H_2^{18}O$ slope	3.10	3.09	2.82	2.83	3.20

The profiles were obtained with $\xi = 1$ (see Eq. (47)) and an equilibrium (linear) temperature profile.

are also very close, with a slightly deeper peak, a higher slope in the liquid phase and a lower slope in the vapour phase, than for the two previous cases. The last case takes into account the full definition of soil vapour diffusivity proposed by Mélayah et al. (1996). This formula leads to a smaller peak concentration and a higher slope both in the liquid and vapour phases than all the other cases. Once again it appears that there is no objective criteria allowing to select one formulation as compared to the others.

7. Example of numerical results in non-steady state

The last part of the paper illustrates the ability of the model to describe non-steady state conditions. Validity of the results is assessed in the second part of the paper (Braud et al., 2004) using two laboratory data sets. In the simulation, we used the same conditions as in Section 6.2, with an enhancement factor $\xi = 1$ and a kinetic fractionation factor defined in Eq. (33). The only difference is that instead of a constant water supply imposed at the bottom of the soil column, a gravitational flux (i.e. a flux equal to the hydraulic conductivity) was considered. Fig. 4 shows the time evolution of the volumetric water content (left) and oxygen 18 isotopic ratio (right) profiles at various times. The steady state equilibrium profile described in Section 6.2 is also shown (stars).

Fig. 4 (left) shows a rapid drying of the soil surface and after one day, the soil moisture content close to the surface is 0.039 $m^3\ m^{-3}$. Deeper soil water content is also depleted due to deep drainage. The process continues as long as the soil dries until the soil surface reaches a moisture content of 0.032 $m^3\ m^{-3}$, corresponding to a matric potential in equilibrium with the air—see Eq. (46). This water content corresponds to the vertical part of the profile close to the surface. The model outputs include all the components of the water and isotope fluxes both in the liquid and in the vapour phases. We can therefore identify that the depth with a sharp variation in the moisture content corresponds to the evaporation front, i.e. the depth where the water vapour flux becomes dominant as compared to the liquid flux (both being oriented upward). This depth also corresponds to the peak in the isotope concentration profile. However, this evaporation front must not be confounded with the so-called 'zero-flux plane' identified using tensiometers and associated with a zero gradient of the hydraulic head. For instance on day 41, the evaporation front takes place at a depth of 2.8 cm, which also corresponds to the depth of the peak isotope concentration and the depth where upwards vapour and liquid water fluxes are equal. On the other hand, the zero-flux plane is located around 75 cm depth. It is the depth where the sign of the total water flux changes, corresponding to a transition from an upward to a downward flux. Consequently, the moisture profile variations above

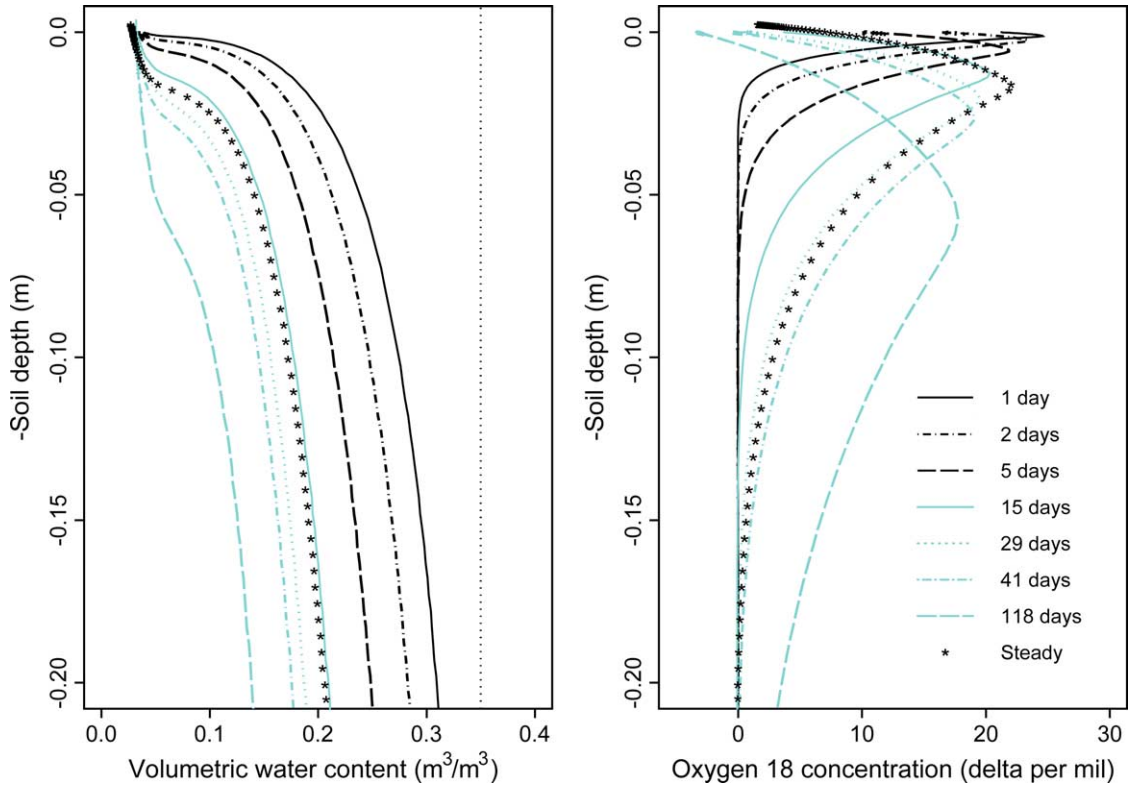

Fig. 4. Volumetric water content (left) and oxygen 18 isotopic concentration (right) profiles for non-steady state conditions; profiles are drawn on days 1, 2, 5, 15, 41 and 118. On the left hand-side graph, the dotted line gives the initial soil moisture content profile. Stars symbols represent the steady state profile corresponding to the same conditions. Simulations were conducted using a 1 m depth soil column, but results are presented for the first 20 cm only for the sake of clarity.

the zero-flux plane can be associated with evaporation whereas the moisture profile variations below the zero-flux plane contribute to deep percolation. Note also that even if the evaporation front takes place at 2.8 cm depth, the soil layer participating in the evaporation process extends well beyond that depth (down to 75 cm depth).

The time evolution of the oxygen 18 isotopic ratio profiles shows a very rapid increase of the surface concentration, with the appearance of a peak around 12 h (not shown). Before 12 h, the surface concentration increases and when the soil surface becomes so dry that water vapour flux becomes dominant, the mechanism of vapour return appears. This time corresponds to the beginning of the so-called second drying phase in the evaporation process (Jackson et al., 1974). As long as the soil dries, the surface isotope concentration decreases towards the value of the atmospheric vapour, the peak decreases and the depth of the maximum increases due to liquid diffusion.

In Fig. 4, we have also plotted (stars) the steady state profiles described in Section 6.2. The soil moisture content almost coincides with that of time 15 days in the non-steady state case. However, the corresponding oxygen 18 concentration profiles are slightly different. The steady state peak shows a higher enrichment and is found at a deeper depth than the non-steady state profile. The instantaneous surface evaporation flux was 1.59×10^{-5} kg m^{-2} s^{-1} on day 15 whereas it was 0.982×10^{-5} kg m^{-2} s^{-1} for the steady state case. On day 29 non-steady state profile corresponds to a similar instantaneous surface evaporation flux (0.982×10^{-5} kg m^{-2} s^{-1}) as that in the steady state case. However, soil moisture is lower than for the steady state case. The oxygen 18 isotopic ratio profile shows a lower maximum and a deeper peak.

The results presented in this section are very close to those shown by Mathieu and Bariac (1996). All these results give confidence in our modelling approach, although the comparison with measurements is the only way to fully validate it.

8. Conclusions

This paper presents a bare soil model able to solve simultaneously the coupled heat, water and stable isotope transport equations. It is based on an existing SVAT model to which an isotope transport module was added. The transport equation calculates the liquid isotope concentration and assumes that the vapour is in equilibrium with the liquid phase. Both diffusive and convective transport are included. Likelihood tests and comparison with analytical solutions both for the saturated and non-saturated conditions showed the consistency of the model, with a good agreement between numerical and analytical results. This first verification validated the choice performed for the basic equations and the numerical discretisation of the problem. The results also showed the importance of using fully coupled heat and water transport equations, due to the relatively large influence of water movement induced by temperature gradients on isotope species concentrations. A resolution of the heat transport equation is also necessary (rather than the use of prescribed soil temperature profiles) in order to get results consistent with the energy balance within the soil.

The most difficult task was the formulation of the surface isotope flux, and especially of the resistance to isotope transport between the soil surface and the atmosphere, which depend on the kinetic fractionation factor. In the literature, various formulae were proposed. We tried to make a rigorous analysis of these formulations. They all were included as possible options within the model. Preliminary sensitivity tests, based on some idealised cases, showed the sensitivity of isotope concentration profiles to this formulation, especially for soil saturated conditions. Hypotheses neglecting molecular diffusion lead to large values of the slope of the $HDO/H_2^{18}O$ relationship, whereas the slope is much smaller when only molecular diffusion is taken into account. On the other hand, both hypotheses led to close slopes under non-saturated conditions. The tests presented in this paper use synthetic data and it is consequently difficult to draw conclusions on the 'best' formula to use. Furthermore, most of the formula were derived using wind tunnel experiments and/or for free water conditions. On the other hand, the comparison with laboratory data performed in the second part of the paper allows to go a step further in the assessment of the validity of the different formula (see Braud et al., 2004).

As compared to previous modelling work, our approach leads to a more general formulation including (i) a fully coupled heat, water and isotope transport model, (ii) the possibility to solve the surface energy balance (although not used in this paper), (iii) a clearer view of the various hypotheses which can be retained for the formulation of the surface isotope flux (isotopic equilibrium between the liquid and vapour phases, even under non-saturated conditions; choice of the kinetic fractionation factor) and of their consequences on simulated isotopic enrichment and slopes of the $HDO/H_2^{18}O$ relationship and (iv) the model has the potential to be applied under field conditions with time varying climate data and to take into account vegetation influence on evapotranspiration processes.

The companion paper (Braud et al., 2004) presents the first assessment of the bare soil model using two existing laboratory column data sets, collected on two contrasting soils (a coarse soil and a fine soil).

Acknowledgements

This study was funded by the French PNRH (Programme National de Recherche en Hydrologie et Environnement), a component of the Programme National/ACI Ecosphère Continentale.

Appendix A. List of symbols

Symbols related to water and heat transfer

C_h capillary capacity (m^{-1})
c_p specific heat at constant pressure ($J\,kg^{-1}\,K^{-1}$)
C_T volumetric heat capacity ($J\,m^{-3}\,K^{-1}$)

D_{ch} isothermal vapour conductivity (W m^{-2})
D_{cT} apparent thermal conductivity (W m^{-1} K^{-1})
D_{mh} isothermal moisture conductivity (m s^{-1})
D_{mT} thermal vapour diffusivity (m^2 s^{-1} K^{-1})
D_v vapour diffusivity of water vapour in air (m^2 s^{-1})
D_{vh} isothermal vapour diffusivity (kg m^{-2} s^{-1})
D_{vT} vapour diffusivity associated with temperature gradients (kg m^{-1} s^{-1} K^{-1})
E evaporation from the ground (W m^{-2})
E_p potential evaporation (kg m^{-2} s^{-1})
g acceleration of gravity (m s^{-2})
G surface soil heat flux (W m^{-2})
h soil matric potential of water (m)
h_a air surface relative humidity (–)
h_a' air surface relative humidity normalised at the soil surface temperature (–)
h_g scale exponent for soil matric potential in the Van Genuchten model (m)
h_j soil matric potential of water of layer j (m)
h_s soil surface relative humidity (–)
h_u soil relative humidity (–)
H sensible heat flux from the ground (W m^{-2})
K liquid hydraulic conductivity (m s^{-1})
K_{sat} saturated liquid hydraulic conductivity (m s^{-1})
L_v latent heat of vaporization (J kg^{-1})
m shape parameter of the Van Genuchten model (–)
n shape parameter of the Van Genuchten model (–)
n_{soil} soil porosity (–)
M_w molar mass of water (kg) $M_w = 0.018$ kg
N_w number of moles of water (mol)
p_{atm} surface atmospheric pressure (Pa)
P_g precipitation at the ground surface (m s^{-1})
q_a specific humidity of air at level z_a (kg kg^{-1})
q_l liquid water flux (m s^{-1})
q_s soil surface specific humidity (kg kg^{-1})
q_v vapour water flux (m s^{-1})
Q_{mg} Darcian non-isothermal flow crossing the soil surface (kg m^{-2} s^{-1})
r_a aerodynamic resistance between level z_a and the soil surface (s m^{-1})
r_{am} molecular resistance between level z_a and the soil surface (s m^{-1})
r_{aT} turbulent resistance between level z_a and the soil surface (s m^{-1})
R perfect mass constant for water vapour (J kg^{-1})
RA incoming long wave radiation (W m^{-2})
RG incoming solar radiation (W m^{-2})
Rn net radiation (W m^{-2})
t time (s)
T soil temperature (K)
T_a air temperature at level z_a (K)
T_j soil temperature of layer j (K)
T_s soil surface temperature (K)
u^* friction velocity (m s^{-1})
U_a wind speed at level z_a (m s^{-1})
z vertical coordinate (m)
z_a height of the atmosphere reference level (m)
z_{om} roughness length for momentum (m)
α bare soil albedo (–)
ε bare soil emissivity (–)
η shape parameter of hydraulic conductivity curve (–)
λ soil thermal conductivity (W m^{-1} K^{-1})
Λ hydrodynamic dispersivity (m)
θ_l liquid volumetric water content (m^3 m^{-3})
θ_r residual liquid volumetric water content (m^3 m^{-3})
θ_s soil surface volumetric water content (m^3 m^{-3})
θ_{sat} saturated volumetric water content (m^3 m^{-3})
θ_v vapour volumetric water content (m^3 m^{-3})
ν air kinematic viscosity (m^2 s^{-1})
ρ_a air volumetric mass (kg m^{-3})
ρ_v water vapour volumetric mass (kg m^{-3})
ρ_{sat}^v saturated water vapour volumetric mass (kg m^{-3})
ρ_w liquid water volumetric mass (kg m^{-3})
σ Stephan–Boltzmann constant (5.67×10^{-8} W m^{-2} K^{-4})
τ soil tortuosity (–)
ξ temperature gradient enhancement factor

Symbols related to water stable isotope transport

C_i concentration of isotopic species i (kg m^{-3})
C_i^l liquid concentration of isotopic species i (kg m^{-3})
C_i^v vapour concentration of isotopic species i (kg m^{-3})
C_{ia}^v atmospheric vapour concentration of isotopic species i at reference level z_a (kg m^{-3})
C_{is}^v soil surface vapour concentration of isotopic species i (kg m^{-3})
$D_i^{l^*}$ total liquid diffusivity for isotope i (m^2 s^{-1})

$D_i^{v^*}$ total vapour diffusivity for isotope i ($m^2\ s^{-1}$)
D_i^{lo} liquid diffusivity of isotope i ($m^2\ s^{-1}$)
D_i^v vapour diffusivity of isotope i in air ($m^2\ s^{-1}$)
E_i surface isotopic flux for species i ($kg\ m^{-2}\ s^{-1}$)
m_i mass of isotopic species i (kg)
m_T total mass of water (kg)
M_i molar mass of isotopic species i (kg) M_i= 0.019 kg for HDO, M_i=0.020 kg for $H_2^{18}O$.
n_a, n_s parameters used in the definition of the n'_K exponent (–)
n_D exponent used in the definition of the total isotope vapour diffusivity (–)
n_K exponent used in the definition of the kinetic fractionation factor (–)
$n_K{}'$ modified exponent used in the definition of the kinetic fractionation factor (–)
N_i number of moles of isotopic species i (mol)
q_i total isotope flux for species i ($kg\ m^{-2}\ s^{-1}$)
q_i^l liquid total isotope flux for species i ($kg\ m^{-2}\ s^{-1}$)
q_i^v vapour total isotope flux for species i ($kg\ m^{-2}\ s^{-1}$)
r_i resistance to isotopic species transfer between the soil surface and the atmosphere ($s\ m^{-1}$)
R_i isotopic ratio of isotopic species i (–)
R_{ia}^v atmospheric vapour isotopic ratio of isotopic species i at reference level z_a (–)
R_{is}^l soil surface liquid isotopic ratio of isotopic species i (–)
R_{is}^v soil surface vapour isotopic ratio of isotopic species i (–)
α_i^* isotopic equilibrium fractionation factor for species i (–)
$\alpha_{\tau K}$ isotopic kinetic fractionation factor for species i (–)
β_i^* factor relating liquid and vapour isotope concentration for species i (–)
δ_i isotopic ratio of isotopic species i (delta unit)
δ_{ia}^v atmospheric vapour isotopic ratio of isotopic species i at reference level z_a (delta unit)

Appendix B. Summary of the main equations solved in the SiSPAT SVAT model for bare soil

All the symbols are defined in Appendix A

Model compartment	Equations	Outputs of the compartment
Atmosphere	Forcing T_a, q_a, U_a, RG, RA, P or E_p	
Soil–atmosphere interface	$Rn = H + L_v E + G$ $E + Q_{mg} - P_g/\rho_w = 0$ $Rn = (1-\alpha)RG + \varepsilon(RA - \sigma T_s^4)$ $E = -\rho_a(q_a - q_s)/r_a$ $H = -\rho_a c_p(T_a - T_s)/r_a$	q_s, T_1
Soil	Upper boundary condition: Q_{mg}, G $C_h \frac{\partial h}{\partial t} = \frac{\partial}{\partial z}\left(D_{mh}\frac{\partial h}{\partial z} + D_{mT}\frac{\partial T}{\partial z} - K\right)$ $C_T \frac{\partial T}{\partial t} = \frac{\partial}{\partial z}\left(D_{ch}\frac{\partial h}{\partial z} + D_{cT}\frac{\partial T}{\partial z}\right)$ $D_{mh} = K + D_{vh}/\rho_w$ $D_{mT} = D_{vT}/\rho_w$ $D_{ch} = L_v D_{vh}$ $D_{cT} = \lambda$ Lower boundary condition: T prescribed, h prescribed or flux prescribed or gravitational flux	hj, Tj, j=1,…,N

Appendix C. Physical relationships

R_{ref} is a reference value for the isotopic ratio (Vienna Standard Mean Ocean Water—SMOW) the value of which is given by Gonfiantini (1978):

$R_{ref} = 155.76 \times 10^{-6}$ for HDO and $R_{ref} = 2005.2 \times 10^{-6}$ for $H_2^{18}O$

The liquid diffusivity of isotope i, D_i^{lo} ($m^2\ s^{-1}$), depends on temperature T (K) following

$$D_i^{lo} = a_i 1 \times 10^{-9} \exp\left(-\frac{535400}{T^2} + \frac{1393.3}{T} + 2.1876\right) \quad (C.1)$$

a_i is a constant depending on the isotopic species. We used:

$a_i = 0.9833$ for HDO and $a_i = 0.9669$ for $H_2^{18}O$

The vapour diffusivity of water in air, D_v ($m^2\ s^{-1}$), depends on temperature T (K) and air pressure p_{atm} (Pa)

$$D_v = 2.17 \times 10^{-5} \frac{10^5}{p_{atm}} \left(\frac{T}{273.16}\right)^{1.88} \quad (C.2)$$

D_i^v ($m^2\ s^{-1}$) is the diffusivity of isotopic vapour in air which is obtained as

$$D_v = b_i D_i^v \quad (C.3)$$

where the value of the constant b_i determined by Merlivat (1978a):

$b_i = 1.0251$ for HDO and $b_i = 1.0285$ for $H_2^{18}O$

The liquid–vapour isotopic fractionation factor at equilibrium, α_i^*(–), is given by Majoube (1971) as a function of temperature T (K)

$$\alpha_i^* = \exp\left(-\left[\frac{a}{T^2} + \frac{b}{T} + c\right]\right) \quad (C.4)$$

The numerical values of the a, b, c coefficients are:

$$\begin{cases} a = 24844 \\ b = -76.248 \quad \text{for HDO} \quad \text{and} \\ c = 0.052612 \end{cases}$$

$$\begin{cases} a = 1137 \\ b = -0.4156 \quad \text{for } H_2{}^{18}O \\ c = -0.0020667 \end{cases}$$

Appendix D. Numerical discretisation

Finite differences were used. Equations were discretized using the local mass balance method (see Fig. D1). At each time step, the isotope species transport is calculated once the coupled heat and water transport equations have been first solved. Solution of these coupled equations provides the values of soil temperature, soil water matric potential and water content profiles at the new time step. Consequently, storage and transport coefficients given by Eqs. (20)–(22) and appearing in the isotope transport equation (Eq. (19)) can be evaluated at the new time step.

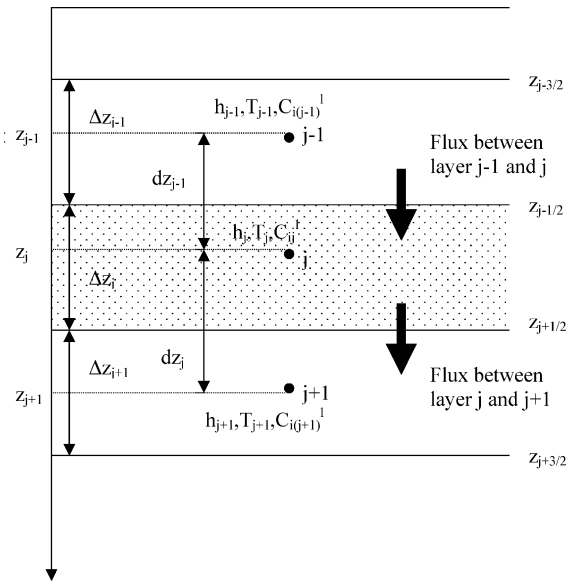

Fig. D1. Definition of the layers used for the discretisation of the mass balance equations.

D.1. Discretisation for layers $2 \le j \le N-1$

For layer j, the Eq. (19) is integrated between depths $z_{j-1/2}$ and $z_{j+1/2}$ and time t^k and t^{k+1} ($\Delta t^{k+1} = t^{k+1} - t^k$)

$$\int_{\Delta t^{k+1}} \int_{z_{j-1/2}}^{z_{j+1/2}} \frac{\partial[\Theta_i C_i^l]}{\partial t} dz\, dt$$

$$= \int_{\Delta t^{k+1}} \int_{z_{j-1/2}}^{z_{j+1/2}} \frac{\partial}{\partial z}\left[D_i^{lv^*} \frac{\partial C_i^l}{\partial z} - Q_i^{lv^*} C_i^l\right] dz\, dt \quad (D.1)$$

Integrals on the left-hand side are inverted and by using the theorem of the mean and an implicit

linearisation, Eq. (D.1) becomes:

$$\int_{z_{j-1/2}}^{z_{j+1/2}} [\Theta_i C_i^{\mathrm{l}}]^{k+1} - [\Theta_i C_i^{\mathrm{l}}]^{k} \mathrm{d}z = \int_{\Delta t^{k+1}} \left(\left[D_i^{\mathrm{lv}^*} \frac{\partial C_i^{\mathrm{l}}}{\partial z} - Q_i^{\mathrm{lv}^*} C_i^{\mathrm{l}} \right]_{z_{j+1/2}} - \left[D_i^{\mathrm{lv}^*} \frac{\partial C_i^{\mathrm{l}}}{\partial z} - Q_i^{\mathrm{lv}^*} C_i^{\mathrm{l}} \right]_{z_{j-1/2}} \right) \mathrm{d}t \tag{D.2}$$

After a second implicit linearisation and with $\Delta z_j = (z_{j+1/2} - z_{j-1/2})$ (thickness of layer j) and $\mathrm{d}z_j = (z_{j+1} - z_j)$ (thickness between nodes j and $j+1$), the final discretized equation reads for $2 \le j \le N-1$ where N is the total number of nodes:

$$([\Theta_i C_i^{\mathrm{l}}]^{k+1} - [\Theta_i C_i^{\mathrm{l}}]^{k}) \Delta z_j = \left(\left[D_i^{\mathrm{lv}^*} \frac{\partial C_i^{\mathrm{l}}}{\partial z} - Q_i^{\mathrm{lv}^*} C_i^{\mathrm{l}} \right]_{z_{j+1/2}}^{t^{k+1}} - \left[D_i^{\mathrm{lv}^*} \frac{\partial C_i^{\mathrm{l}}}{\partial z} - Q_i^{\mathrm{lv}^*} C_i^{\mathrm{l}} \right]_{z_{j-1/2}}^{t^{k+1}} \right) \Delta t^{k+1} \tag{D.3}$$

To get the final discretized equation, vertical gradients of concentrations are approximated using finite differences, leading to:

$$([\Theta_{ij}^{k+1} C_{ij}^{\mathrm{l}(k+1)}] - [\Theta_{ij}^{k} C_{ij}^{\mathrm{l}k}]) \frac{\Delta z_j}{\Delta t^{k+1}} = D_{i(j+1/2)}^{\mathrm{lv}^*(k+1)} \frac{C_{i(j+1)}^{\mathrm{l}(k+1)} - C_{ij}^{\mathrm{l}(k+1)}}{dz_j} - Q_{i(j+1/2)}^{\mathrm{lv}^*(k+1)} (C_i^{\mathrm{l}(k+1)})_{j+1/2} - D_{i(j-1/2)}^{\mathrm{lv}^*(k+1)} \frac{C_{ij}^{\mathrm{l}(k+1)} - C_{i(j-1)}^{\mathrm{l}(k+1)}}{dz_{j-1}} + Q_{i(j-1/2)}^{\mathrm{lv}^*(k+1)} (C_i^{\mathrm{l}(k+1)})_{j-1/2} \tag{D.4}$$

In Eq. (D.4), transport coefficients $D_i^{\mathrm{lv}*}$ and isotopic liquid concentration C_i^{l} must be evaluated at the inter-nodes, while they are known at the nodes. Arithmetic means are used for that purpose, leading to:

$$(C_i^{\mathrm{l}(k+1)})_{j-1/2} = \frac{C_{i(j-1)}^{\mathrm{l}(k+1)} + C_{ij}^{\mathrm{l}(k+1)}}{2} \tag{D.5}$$

$$(C_i^{\mathrm{l}(k+1)})_{j+1/2} = \frac{C_{ij}^{\mathrm{l}(k+1)} + C_{i(j+1)}^{\mathrm{l}(k+1)}}{2} \tag{D.6}$$

$$D_{i(j-1/2)}^{\mathrm{lv}^*(k+1)} = \frac{D_{i(j-1)}^{\mathrm{lv}^*(k+1)} + D_{ij}^{\mathrm{lv}^*(k+1)}}{2} \tag{D.7}$$

$$D_{i(j+1/2)}^{\mathrm{lv}^*(k+1)} = \frac{D_{ij}^{\mathrm{lv}^*(k+1)} + D_{i(j+1)}^{\mathrm{lv}^*(k+1)}}{2} \tag{D.8}$$

For the $Q_i^{\mathrm{lv}*}$ coefficient, the following approximation of Eq. (21) was retained:

$$Q_{i(j-1/2)}^{\mathrm{lv}^*(k+1)} = q_{j-1/2}^{\mathrm{l}} + q_{j-1/2}^{\mathrm{v}} \frac{\beta_{i(j-1)}^{*(k+1)} + \beta_{ij}^{*(k+1)}}{2} - \frac{D_{i(j-1)}^{\mathrm{v}^*(k+1)} + D_{ij}^{\mathrm{v}^*(k+1)}}{2} \frac{\beta_{ij}^{*(k+1)} - \beta_{i(j-1)}^{*(k+1)}}{dz_{j-1}} \tag{D.9}$$

$$Q_{i(j+1/2)}^{\mathrm{lv}^*(k+1)} = q_{j+1/2}^{\mathrm{l}} + q_{j+1/2}^{\mathrm{v}} \frac{\beta_{i(j+1)}^{*(k+1)} + \beta_{ij}^{*(k+1)}}{2} - \frac{D_{i(j+1)}^{\mathrm{v}^*(k+1)} + D_{ij}^{\mathrm{v}^*(k+1)}}{2} \frac{\beta_{i(j+1)}^{*(k+1)} - \beta_{ij}^{*(k+1)}}{dz_j} \tag{D.10}$$

It takes advantage of the liquid and vapour water fluxes being calculated at the internodes by the model.

Eq. (D.4) can be rewritten as a function of liquid isotopic concentrations at the various nodes, leading to

$$A1_{ij} C_{i(j-1)}^{\mathrm{l}(k+1)} + A2_{ij} C_{ij}^{\mathrm{l}(k+1)} + A3_{ij} C_{i(j+1)}^{\mathrm{l}(k+1)} = B_{ij} \quad 2 \le j \le N-1 \tag{D.11}$$

where

$$A1_{ij} = -\frac{D_{i(j-1/2)}^{\mathrm{lv}^*(k+1)}}{\mathrm{d}z_{j-1}} - \frac{Q_{i(j-1/2)}^{\mathrm{lv}^*(k+1)}}{2} \tag{D.12}$$

$$A2_{ij} = \frac{\Delta z_j}{\Delta t^{k+1}} \Theta_{ij}^{k+1} + \frac{D_{i(j+1/2)}^{\mathrm{lv}^*(k+1)}}{\mathrm{d}z_j} + \frac{Q_{i(j+1/2)}^{\mathrm{lv}^*(k+1)}}{2} + \frac{D_{i(j-1/2)}^{\mathrm{lv}^*(k+1)}}{\mathrm{d}z_{j-1}} - \frac{Q_{i(j-1/2)}^{\mathrm{lv}^*(k+1)}}{2} \tag{D.13}$$

$$A3_{ij} = -\frac{D_{i(j+1/2)}^{\mathrm{lv}^*(k+1)}}{\mathrm{d}z_j} + \frac{Q_{i(j+1/2)}^{\mathrm{lv}^*(k+1)}}{2} \quad \text{(D.14)}$$

$$B_{ij} = \frac{\Delta z_j}{\Delta t^{k+1}} \Theta_{ij}^{k} C_{ij}^{\mathrm{l}k} \quad \text{(D.15)}$$

D.2. Discretisation for layer j=1

For the first layer, the value of the above coefficients depends on the choice of the boundary condition type.

For a known value of the liquid isotopic concentration C_{is}^{l}, coefficients read:

$$A1_{i1} = 0, \quad A2_{i1} = 1, \quad A3_{i1} = 0, \quad B_{i1} = C_{is}^{\mathrm{l}} \quad \text{(D.16)}$$

If a prescribed value of the liquid isotope flux E_i (kg m^{-2} s^{-1}) is imposed at the soil surface, coefficients become:

$$A1_{i1} = 0 \quad \text{(D.17)}$$

$$A2_{i1} = \frac{\Delta z_j}{\Delta t^{k+1}} \Theta_{i1}^{k+1} + \frac{D_{i(1+1/2)}^{\mathrm{lv}^*(k+1)}}{\mathrm{d}z_1} + \frac{Q_{i(1+1/2)}^{\mathrm{lv}^*(k+1)}}{2} \quad \text{(D.18)}$$

$$A3_{i1} = -\frac{D_{i(1+1/2)}^{\mathrm{lv}^*(k+1)}}{\mathrm{d}z_1} + \frac{Q_{i(1+1/2)}^{\mathrm{lv}^*(k+1)}}{2} \quad \text{(D.19)}$$

$$B_{i1} = \frac{\Delta z_1}{\Delta t^{k+1}} \Theta_{i1}^{k} C_{is}^{\mathrm{l}k} + E_i \quad \text{(D.20)}$$

D.3. Discretisation for layer j=N

At the bottom of the soil profile, a known value of the liquid isotopic concentration C_{iN}^{l} leads to the following expressions of the coefficients:

$$A1_{iN} = 0, \quad A2_{iN} = 1, \quad A3_{iN} = 0, \quad B_{iN} = C_{iN}^{\mathrm{l}} \quad \text{(D.21)}$$

For a prescribed value of the isotope flux $q_{iN} = q_N C_{iN}^{\mathrm{l}k}$ (kg m^{-2} s^{-1}), coefficients read:

where

$$A1_{i1} = -\frac{D_{i(N-1/2)}^{\mathrm{lv}^*(k+1)}}{\mathrm{d}z_N} - \frac{Q_{i(N-1/2)}^{\mathrm{lv}^*(k+1)}}{2} \quad \text{(D.22)}$$

$$A2_{iN} = \frac{2\Delta z_N}{\Delta t^{k+1}} \Theta_{iN}^{k+1} + \frac{D_{i(N-1/2)}^{\mathrm{lv}^*(k+1)}}{\mathrm{d}z_{N-1}} - \frac{Q_{i(N-1/2)}^{\mathrm{lv}^*(k+1)}}{2} \quad \text{(D.23)}$$

$$A3_{i1} = 0 \quad \text{(D.24)}$$

$$B_{iN} = \frac{2\Delta z_N}{\Delta t^{k+1}} \Theta_{iN}^{k} C_{iN}^{\mathrm{l}k} - q_{iN} \quad \text{(D.25)}$$

D.4. Final linear system to be solved

The above discretized equations can finally be written in a matrix form

$$[A][X] = [B] \quad \text{(D.26)}$$

where

$$[X] = \begin{bmatrix} C_{i1}^{\mathrm{l}(k+1)} \\ C_{i2}^{\mathrm{l}(k+1)} \\ \cdot \\ C_{ij}^{\mathrm{l}(k+1)} \\ \cdot \\ C_{iN}^{\mathrm{l}(k+1)} \end{bmatrix} \quad \text{and} \quad [B] = \begin{bmatrix} B_{i1} \\ B_{i2} \\ \cdot \\ B_{ij} \\ \cdot \\ B_{iN} \end{bmatrix}$$

The matrix $[A]$ is tridiagonal:

$$[A] = \begin{bmatrix} A2_{i1} & A3_{i1} & & & & & \\ A1_{i2} & A2_{i2} & A3_{i2} & & & & \\ & \cdot & \cdot & \cdot & & & \\ & & A1_{ij} & A2_{ij} & A3_{ij} & & \\ & & & \cdot & \cdot & \cdot & \\ & & & & A1_{i(N-1)} & A2_{i(N-1)} & A3_{i(N-1)} \\ & & & & & A1_{iN} & A2_{iN} \end{bmatrix}$$

This linear system is easily solved by using the Thomas algorithm proposed by Douglas et al. (1959) and given in details in Touma (1984). It provides the values of the liquid isotopic concentration at all the nodes of the soil. The vapour isotopic concentration can be deduced from Eq. (14) and the values converted to delta notations using Eqs. (5) and (6).

References

Auriault, J.L., Adler, P.M., 1995. Taylor dispersion in porous media: analysis by multiple scale expansions. Advances in Water Resources 18 (4), 217–226.

Bariac, T., Gonzalez-Dunia, J., Tardieu, F., Teissier, D., Mariotti, A., 1994. Variabilité spatiale de la composition isotopique de l'eau (^{18}O, ^{2}H) au sein des organes des plantes aériennes: approche en conditions contrôlées. Chemical Geology 115, 307–315.

Bariac, T., Maillard, P., Bonnefond, J.M., 1995. Apports de la méthodologie isotopique à l'analyse du transfert de l'eau dans le continuum sol-plante-atmosphère, Actes de l'Ecole Chercheurs INRA en Bioclimatologie, Le Croisic 3–7 Avril 1995. Tome 1: De la plante au couvert végétal, Editions INRA: 593–616.

Barnes, C.J., Allison, G.B., 1983. The distribution of deutérium and ^{18}O in dry soils. 1. Theory. Journal of Hydrology 60, 141–156.

Barnes, C.J., Allison, G.B., 1984. The distribution of deutérieum and ^{18}O in dry soils. 3. Theory for no isothermal water movement. Journal of Hydrology 74, 119–135.

Boulet, G., Braud, I., Vauclin, M., 1997. Study of the mechanisms of evaporation under arid conditions using a detailed model of the soil–atmosphere continuum. Journal of Hydrology 193, 114–141.

Braud, I., 2000. SiSPAT User's manual, Version 3.0, 106 pp. Available at http://www.lthe.hmg.inpg.fr/Sispat

Braud, I., 2002. SiSPAT User's Manual Update, version 4.0, 13 pp.

Braud, I., Dantas-Antonino, A.C., Vauclin, M., Thony, J.L., Ruelle, P., 1995. A simple soil–plant–atmosphere transfer model (SiSPAT): development and field verification. Journal of Hydrology 166, 213–250.

Braud, I., Bessemoulin, P., Monteny, B., Sicot, M., Vandervaere, J.P., Vauclin, M., 1997. Unidimensional modelling of a fallow savannah during the Hapex-Sahel experiment using the SiSPAT model. Journal of Hydrology 188–189, 912–945.

Braud, I., Bariac, T., Vauclin, M., Boujamlaoui, Z., Gaudet, J.P., Biron, Ph., Richard, P., 2004. SiSPAT-Isotope, a coupled heat, water and stable isotope (HDO and $H_2^{18}O$) transport model for bare soil. Part II. Evaluation and sensitivity tests using two laboratory data sets. Journal of Hydrology, doi:10.1016/j.jhydrol.2004.12.012

Brooks, R.H., Corey, A.T., 1964. Hydraulic properties of porous media, Hydrology paper, 3, Colorado State University, Fort Collins, 27 pp.

Brutsaert, W., 1982. Evaporation into the Atmosphere. Kluwer, Dordrecht. 299 pp.

Burdine, N.T., 1953. Relative permeability calculation from size distribution data. Transactions of AIME 198, 71–78.

Calvet, J.C., Bessemoulin, P., Berne, C., Braud, I., Courault, D., Fritz, N., Gonzalez-Sosa, E., Goutorbe, J.P., Haverkamp, R., Jaubert, G., Kergoat, L., Lachaud, G., Laurent, J.P., Mordelet, P., Noilhan, J., Olioso, A., Péris, P., Roujean, J.L., Thony, J.L., Tosca, C., Vauclin, M., Vignes, D., 1999. MUREX: a land-surface field experiment to study the annual cycle of the energy and water budgets. Annales Geophysicae 17 (6), 838–854.

Cappa, C.D., Hendricks, M.B., DePaolo, D.J., Cohen, R.C., 2003. Isotopic fractionation of water during evaporation. Journal of Geophysical Research 108 (D16), 4525.

Celia, M.A., Bouloutas, E.T., Zarba, R.L., 1990. A general mass-conservative numerical solution for the unsaturated flow equation. Water Resources Research 26 (7), 1483–1496.

Craig, H., Gordon, L.I., 1965. Deuterium and oxygen 18 variations in the ocean and the marine atmosphere, Proceedings of the Conference on the Stable Isotopes in Oceanographic Studies and Paleotemperatures. Laboratorie Geologia Nuclear, Pisa, Italy, pp. 9–130.

Douglas, J., Peaceamn, D.W., Rachford, H.H., 1959. A method for calculating multi-dimensional immiscible displacement. Petroleum Transactions of AIME 216, 297–308.

Gat, J.R., 1981. Lakes. In: Gat, J.R., Gonfiantin, R. (Eds.), Stable Isotope Hydrology: Deuterium and Oxygen 18 in the Water Cycle Technical Reports series no. 210. IAEA, Vienna, pp. 203–219.

Gonfiantini, R., 1978. Standards of stable isotope measurement in natural compounds. Nature 271, 534–536.

Gonfiantini, R., 1986. Environmental isotopes in lake studies. In: Fritz, P., Fontes, J.C. (Eds.), Handbook of Environmental Isotope Geochemistry, vol. 2. Elsevier, Amsterdam, Netherlands, pp. 113–167.

Gonzalez-Sosa, E., Braud, I., Thony, J.L., Vauclin, M., Bessemoulin, P., Calvet, J.C., 1999. Modelling heat and water exchanges of fallow land covered with plant-residue mulch. Agricultural and Forest Meteorology 97, 151–169.

Gonzalez-Sosa, E., Braud, I., Thony, J.L., Vauclin, M., Calvet, J.C., 2001. Heat and water exchanges of fallow land covered with a plant-residue mulch layer: a modelling study using the three year MUREX data set. Journal of Hydrology 244, 119–136.

Haverkamp, R., Vauclin, M., Touma, J., Wierenga, P.J., Vachaud, G., 1977. A comparison of numerical simulation models for one-dimensional infiltration. Soil Science Society of America Journal 41, 285–294.

Haverkamp, R., Zammit, C., Bouraoui, F., Rajkai, K., Arrué, J.L., 1998. GRIZZLY: Grenoble catalogue of soils, Survey of soil field data and descritpion of particle size, soil water retention and hydraulic conductivity functions, LTHE, BP 53, 38041 Grenoble Cédex 9, France, 117 pp.

Jackson, R.D., Reginato, R.J., Kimball, B.A., Nakayama, F.S., 1974. Diurnal soil–water evaporation: comparison of measured and calculated soil–water fluxes. Soil Science Society of America Journal 38 (6), 861–866.

Majoube, M.A., 1971. Fractionnement en oxygène-18 et en deutérium entre l'eau et sa vapeur. Journal of Chemical Physics 68, 1423–1436.

Mathieu, R., Bariac, T., 1996. A numerical model for the simulation of stable isotope profiles in drying soils. Journal of Geophysical Research 101 (D7), 12685–12696.

Mélayah, A., Bruckler, L., Bariac, T., 1996. Modeling the transport of water stable isotopes in unsaturated soils under natural conditions. 1. Theory. Water Resources Research 32 (7), 2047–2054.

Ménache, M., 1966. Variation de la masse volumique de l'eau en fonction de sa composition isotopique. Extrait des Cahiers Océanogrqphiques, XVIII 6, 1–20.

Merlivat, L., 1978a. Molecular diffusivity of $H_2^{16}O$, $HD^{16}O$ and $H_2^{18}O$ in gases. Journal of Chemical Physics 69, 2864–2871.

Merlivat, L., 1978b. The dependence of bulk evaporation coefficients on air–water interfacial conditions as determined by the isotopic method. Journal of Geophysical Research 83 (C6), 2977–2980.

Merlivat, L., Coantic, M., 1975. Study of the mass transfer at the air–water interface by an isotopic method. Journal of Geophysical Research 80 (24), 3455–3464.

Merlivat, L., Jouzel, J., 1978. Global climatic interpretation of the interpretation of the. Journal of Geophysical Research 84 (C8), 5029–5033.

Olioso, A., Braud, I., Chanzy, A., Courault, D., Demarty, J., Kergoat, L., Lewan, E., Ottlé, C., Prévot, L., Zhao, W., Calvet, J.C., Cayrol, P., Jongschaap, R., Moulin, S., Noilhan, J., Wigneron, J.P., 2002. SVAT modeling over the Alpilles-ReseDA experiment: comparing SVAT models over wheat fields. Agronomie 22, 651–668.

Philip, J.R., 1957. Evaporation, moisture and heat field in the soil. Journal of Meteorology 14, 354–366.

Philip, J.R., De Vries, D.A., 1957. Moisture movement in porous materials under temperature gradients. Transactions of the American Geophysical Union 38, 222–232.

Shurbaji, A.R., Phillips, F.M., 1995. A numerical model for the movement of H_2O, $H_2^{18}O$, and ^2HHO in the unsaturated zone. Journal of Hydrology 171, 125–142.

Stewart, M.K., 1975. Stable isotope fractionation due to evaporation and isotopic exchange of falling waterdrops. Application to atmospheric processes and evaporation of lakes. Journal of Geophysical Research 80, 1133–1146.

Touma, J., 1984. Etude critique de la caractérisation hydrodynamique des sols non saturés: rôle de l'air. Influence de l'écoulement multidimensionnel de l'eau. Thèse de Docteur ès Sciences Physiques, Université Scientifique et Technique de Grenoble, Grenoble, France.

Van Genuchten, M.T., 1980. A closed-form equation for predicting the hydraulic conductivity of unsaturated soils. Soil Science Society of America Journal 44, 892–898.

Vauclin, M., Haverkamp, R., Vachaud, G., 1979. Résolution numérique d'une équation de diffusion non-linéaire. Application à l'infiltration de l'eau dans les sols non saturés, Presses Universitaires de Grenoble, Grenoble, 183 pp.

Walker, C.D., Richardson, S.B., 1991. The use of stable isotopes of water in characterising the source of water in vegetation. Chemical Geology 94, 145–158.

Williams, D.G., Cable, W., Hultine, K., Hoedjes, J.C.B., Yepez, E.A., Simmonneaux, V., El-Raki, S., Boulet, G., de Bruin, H.A.R., Chehbouni, A., Hartogensis, O.K., Timouk, F., 2004. Evapotranspiration components determined by stable isotope, sap flow and eddy covariance techniques. Agricultural and Forest Meteorology 125, 241–258.

Yepez, E.A., Williams, D.G., Russelle, L.S., Guanghui, L., 2003. Partitioning overstory and understory evapotranspiration in a semiarid savanna woodland from the isotopic composition of water vapor. Agricultural and Forest Meteorology 119, 53–68.

Zimmermann, U., Ehhalt, D., Münnich, K.O., 1967. Soil water movement and evapotranspiration: changes in the isotopic composition of the water, Proceedings of the Symposium of Isotopes in Hydrology. IAEA, Vienna, pp. 567–584.